

# Water Resources Research®

## REVIEW ARTICLE

10.1029/2024WR037216

Tongge Jing and Yi Zeng contributed equally to this work.

### Key Points:

- We review hysteresis methods and identify global hotspots for analyzing suspended sediment dynamic during discrete hydrological events
- Combining qualitative and quantitative hysteresis methods effectively classify events and reveal sediment sources and transport processes
- Hysteresis methods face challenges in accuracy and applicability under the growing complexity of future extreme events

### Supporting Information:

Supporting Information may be found in the online version of this article.

### Correspondence to:

N. Fang,  
fnf@ms.iswc.ac.cn

### Citation:



Jing, T., Zeng, Y., Fang, N., Dai, W., & Shi, Z. (2025). A review of suspended sediment hysteresis. *Water Resources Research*, 61, e2024WR037216. <https://doi.org/10.1029/2024WR037216>

Received 1 FEB 2024  
Accepted 10 DEC 2024

© 2024. The Author(s).

This is an open access article under the terms of the [Creative Commons Attribution-NonCommercial-NoDerivs License](#), which permits use and distribution in any medium, provided the original work is properly cited, the use is non-commercial and no modifications or adaptations are made.

## A Review of Suspended Sediment Hysteresis

Tongge Jing<sup>1</sup>, Yi Zeng<sup>1</sup>, Nufang Fang<sup>1,2</sup> , Wei Dai<sup>1</sup>, and Zhihua Shi<sup>2,3</sup> 

<sup>1</sup>State Key Laboratory of Soil Erosion and Dryland Farming on the Loess Plateau, Institute of Soil and Water Conservation, Northwest A&F University, Yangling, PR China, <sup>2</sup>Institute of Soil and Water Conservation, Chinese Academy of Sciences and Ministry of Water Resources, Yangling, PR China, <sup>3</sup>College of Resources and Environment, Huazhong Agricultural University, Wuhan, PR China

**Abstract** The study of sediment-riverflow interactions during discrete hydrological events is vital for enhancing our understanding of the hydrological cycle. Hysteresis analysis, relying on high-resolution, continuous monitoring of suspended sediment concentration (SSC) and discharge (Q) data, is an effective tool for investigating complex hydrological events. It captures differing sediment dynamic at the same discharge level, which results from the asynchrony between the hydrograph and sediment graph during different phases of the event. However, there has been no comprehensive review systematically addressing the utility and significance of hysteresis analysis in soil and water management. This review synthesizes findings from over 500 global studies, providing a detailed examination of current research. We trace the development and application of hysteresis analysis in hydrology, illustrating its role in classifying and characterizing events, as well as uncovering sediment sources and transport mechanisms. Furthermore, hysteresis analysis has proven effective in identifying critical hydrological events, offering valuable insights for targeted watershed management. Our spatiotemporal analysis of global hysteresis research shows that over 70% of studies are located in semi-arid and Mediterranean climate zones, with an increasing focus on alpine and tropical regions due to climate change. This review also highlights critical limitations, including the scarcity of high-resolution data, inconsistent use of quantitative indices, and limited integration of hysteresis patterns into predictive hydrological approaches. Future research should focus on developing region-specific hydrological models that incorporate hysteresis dynamics, along with standardizing methodologies to apply hysteresis analysis across diverse climatic and geomorphic settings.

## 1. Introduction

Suspended sediment (SS) plays a crucial role in hydrological systems, contributing to landform development, ecosystem sustainability, and nutrient transport (Achite & Ouillon, 2016; Vercruyssen et al., 2017). Significant changes in SS dynamics have been observed across various time scales, spanning from decadal trends to episodic events, attributed to the intensification of climate change and human activities (Overeem et al., 2017; Syvitski et al., 2022; Walling, 2006). Examining the relationship between suspended sediment concentration (SSC) and river discharge (Q) is essential for understanding SS dynamics, offering key insights into sediment sources, transport pathways, and deposition processes within fluvial systems (Collins & Walling, 2004; Gao et al., 2018; Rustomji et al., 2008). This relationship becomes especially critical during hydrological events, which have increased in both frequency and intensity in recent years, contributing significantly to overall sediment transport (Rose & Karwan, 2021; Speir et al., 2024; Zarnaghsh & Husic, 2023). Therefore, analyzing the SSC-Q relationships during hydrological events proves invaluable for devising sustainable watershed management strategies.

The traditional sediment rating curve (SRC) method has been widely used in large-scale studies of SSC-Q relationships and is effective under stable conditions, as it estimates SSC based on a power function of Q (Aguilera & Melack, 2018; Gao & Josefson, 2012; Horowitz et al., 2015). However, SRCs often fail to accurately capture the highly variable and nonlinear sediment transport processes that occur during hydrological events (Di Pillo et al., 2023; Pietron et al., 2015; Rodriguez-Blanco et al., 2018; Rose et al., 2018). These limitations are particularly pronounced in dynamic flood conditions, where sediment supply and transport capacity fluctuate between the rising and falling limbs of the hydrograph due to shifting hydrological and geomorphological factors (Coch et al., 2018; Domingo et al., 2021; Dupas et al., 2015; Garcia-Rama et al., 2016; Speir et al., 2024). The inherent variability in the transport rates of water and sediment during hydrological events often leads to lag effects, which traditional SRCs struggle to account for effectively.

The complexity of hydrological events is largely driven by the differential transport rates of water and sediment, which results in lag (Fortesa et al., 2021; Hudson, 2003; Rose & Karwan, 2021; Sammori et al., 2004). To capture these dynamics, researchers since the mid-twentieth century introduced the concept of hysteresis loops, where SSC is plotted against river discharge (Q) over time (Banasik et al., 2005; Banasik & Walling, 1996; Heidele, 1956; Klein, 1984; Rendon-Herrero, 1978; Williams, 1989). This approach reveals variations in sediment transport between the rising and falling limbs of the hydrograph, providing a more nuanced view of sediment dynamic during hydrological events (Baker & Showers, 2019; Lenzi & Marchi, 2000; Ziegler et al., 2014). Hysteresis loops are typically classified into distinct patterns—such as clockwise, counterclockwise, figure-eight, and more complex forms—based on their direction and shape (Baloul et al., 2024; Buendia et al., 2016; Hamshaw et al., 2018; Keesstra et al., 2019; Lloyd et al., 2016a; Oeurng et al., 2010; Pellegrini et al., 2023; Safdar et al., 2024; Zarnaghsh & Husic, 2021). These patterns offer valuable insights into sediment sources, transport pathways, and depositional processes, facilitating a more detailed classification of hydrological events and improving understanding of sediment transport mechanisms (Bowes et al., 2005; Hu et al., 2019; Lefrancois et al., 2007; Rodriguez-Blanco et al., 2018).

Graphical hysteresis loops have been valuable for qualitatively illustrating the temporal relationship between SSC and Q during hydrological events, but they have notable limitations (Buendia et al., 2016; Lannergard et al., 2021; Lefrancois et al., 2007). A primary issue is that the identification of hysteresis patterns often relies on subjective interpretation, which can introduce inconsistencies and reduce analytical precision (Al Sawaf et al., 2024; Herrero et al., 2018; Tolorza et al., 2014). Additionally, graphical loops alone do not provide sufficient quantitative insights into the drivers of different hysteresis patterns, particularly when sediment sources and transport pathways vary across events or between watersheds with distinct hydrological conditions. To address these shortcomings, hydrologists in the early 21st century introduced quantitative indices, such as the hysteresis index (HI) (Langlois et al., 2005). The HI offers a more objective and precise means of quantifying hysteresis loops, with its sign indicating the direction of the loop and its absolute value representing the degree of lag between SSC and Q (Wilcox et al., 2024). Over the years, the calculation methods for the hysteresis index have been refined, improving its accuracy and making it applicable to a broader range of hydrological settings (Aich et al., 2014; Lawler et al., 2006; Zuecco et al., 2016). The combination of qualitative graphical loops and quantitative hysteresis indices has now become an established method in hydrological research, providing a more rigorous and comprehensive framework for analyzing the complex, nonlinear interactions between SSC and Q during hydrological events (Baniya et al., 2024; Doomen et al., 2008; Dupas et al., 2015; Favaro & Lamoureaux, 2015; Liu et al., 2021).

In recent years, the increasing frequency and variability of hydrological events—driven by climate change and human activities—have garnered growing attention from hydrologists (Heathwaite & Bierozza, 2021; Lopez-Tarazon et al., 2009; Zuecco et al., 2016). Despite the recognition of hysteresis analysis as a valuable tool for investigating SSC-Q interactions during such events, systematic evaluations of its application remain limited, particularly concerning the selection and calculation of appropriate hysteresis indices (Gao & Josefson, 2012; Garcia-Comendador et al., 2021; Rovira & Batalla, 2006; Sadeghi et al., 2008a, 2008b; Sadeghi & Saeidi, 2010; Sun et al., 2016). A growing body of research has incorporated hysteresis indices alongside traditional runoff and sediment metrics to assess the influence of environmental factors—such as climate, watershed characteristics, and anthropogenic activities—on flood dynamic (Lopez-Tarazon & Estrany, 2017; Pulley et al., 2019). However, the intricate interplay between these factors, along with the limitations of current quantitative indices in fully capturing the complexity of hydrological events, suggests substantial opportunities for advancing this method.

Hysteresis analysis offers a significant advantage over traditional runoff and sediment metrics by capturing the temporal dynamic throughout the entire process of a hydrological event (Garcia-Rama et al., 2016; Liu et al., 2021; Malutta et al., 2020; Sadeghi et al., 2017). Unlike conventional models, which predominantly focus on conditions at the watershed outlet and often treat internal processes as a “black box,” hysteresis analysis can provide valuable insights into the evolving nature of flood processes (Di Pillo et al., 2023; Geeraert et al., 2015; Ghimire et al., 2024; Shojaeezadeh et al., 2022; Speir et al., 2024). Integrating hysteresis dynamics into contemporary hydrological models holds great potential for overcoming the limitations of traditional approaches, thereby enhancing hydrological event analysis and prediction in future research.

This review synthesizes findings from over 400 studies on hysteresis analysis, focusing on its evolution, current applications in hydrology, and limitations. The primary aim is to offer clearer guidance on the use of hysteresis methods, identify existing research gaps, and propose directions for future research. By emphasizing the integration of hysteresis dynamics into predictive hydrological models, this review seeks to contribute to more robust hydrological event analysis and sediment management in the face of future environment change.

## 2. The Evolution of Methods for SSC-Q Relationship Analysis

The analysis of SSC-Q relationships is essential for understanding sediment transport processes and mechanisms within river systems. By examining how sediment fluctuates with riverflow under varying conditions, researchers can identify key factors that drive sediment mobilization, such as hydrological variability, land-use practices, and geomorphological changes (Doomen et al., 2008; Herrero et al., 2018; Juez et al., 2018; Yibeltal et al., 2023). Furthermore, quantifying the relationship between sediment and riverflow is critical for developing predictive models that forecast sediment yield and aid in managing sediment budgets (Landers & Sturm, 2013; Long et al., 2024). These models are invaluable for projecting future trends and promoting sustainable watershed management. Over the past few decades, methods for analyzing SSC-Q relationships during hydrological events have undergone significant evolution and refinement (Collins, 1981; Gao et al., 2018; Rustomji et al., 2008). Beginning with traditional sediment rating curves, the field has advanced to incorporate both qualitative and quantitative hysteresis analysis, which has become increasingly prominent in hydrological studies of hydrological events (Rose & Karwan, 2021; Zarnaghsh & Husic, 2021). This chapter provides an overview of the historical development of these methods, tracing their progression from early approaches to more advanced techniques, and presents a global perspective on the spatiotemporal distribution of research related to hysteresis analysis.

### 2.1. Sediment Rating Curves

The sediment rating curve (SRC) has been a prevalent method for analyzing the relationship between suspended sediment concentration (SSC) and discharge (Q) in river systems (Collins, 1981; di Cenzo & Luk, 1997; Walling, 1977). Expressed as a power function,  $SSC = aQ^b$ , it defines two parameters:  $a$ , indicating sediment availability, and  $b$ , representing the sediment transport capacity as discharge increases (Banasik & Walling, 1996; Horowitz et al., 2015; Krajewski et al., 2018; Vercruyssen et al., 2017). This empirical model has been widely applied at various temporal scales—annual, monthly, and daily (Ahn & Steinschneider, 2018; Asselman, 1999; Dumitriu, 2020; Irvine & Drake, 1987; Sadeghi et al., 2008a, 2008b, 2019)—providing a practical approach for estimating long-term sediment loads and transport patterns.

However, its limitations become apparent during hydrological events, where rapid fluctuations in discharge and sediment supply introduce significant variability that the SRC model cannot capture (Baloul et al., 2024; De Girolamo et al., 2015; Katebikord et al., 2024; Speir et al., 2024). A key issue is the lag effect, where SSC and Q peaks do not coincide (Banasik et al., 2005; Banasik & Hejduk, 2015; Jansson, 1996, 2002; Jeje et al., 1991). SSC peaks may occur before, during, or after the discharge peak, causing scatter and poor fits to the power function (Rodriguez-Blanco et al., 2010; Stubblefield et al., 2007; Williams, 1989; Yang & Lee, 2018). This asynchronous behavior, particularly in high-intensity floods, undermines the assumption of a steady relationship between sediment and riverflow. Hydrological events also involve dynamic shifts in sediment availability and transport mechanisms, especially between the rising and falling limbs of the flood hydrograph (Lopez-Tarazon et al., 2009; Sidle & Campbell, 1985). The static relationship between SSC and Q fails to account for these changes, leading to inaccurate sediment load estimates and underrepresenting variability in transport processes (Alexandrov et al., 2007; Hapsari et al., 2019; Lopez-Tarazon & Estrany, 2017). This is particularly problematic in watersheds where large, intense floods disproportionately contribute to sediment yield. As a result, more sophisticated approaches are needed to improve sediment load estimation during hydrological events.

### 2.2. Qualitative Analysis of Hysteresis Loops

In the mid-twentieth century, researchers identified discrepancies between hydrograph and sediment graph during hydrological events, particularly in the timing of their peaks (Heidel, 1956; Paustian & Beschta, 1979; Wood, 1977). These lag effects led to the development of hysteresis loops, which plot SSC against Q over time (Collins, 1981; Grimshaw & Lewin, 1980). Initially, hysteresis loops were simple graphical tools that highlighted the timing differences between sediment and riverflow, revealing variability in sediment transport during

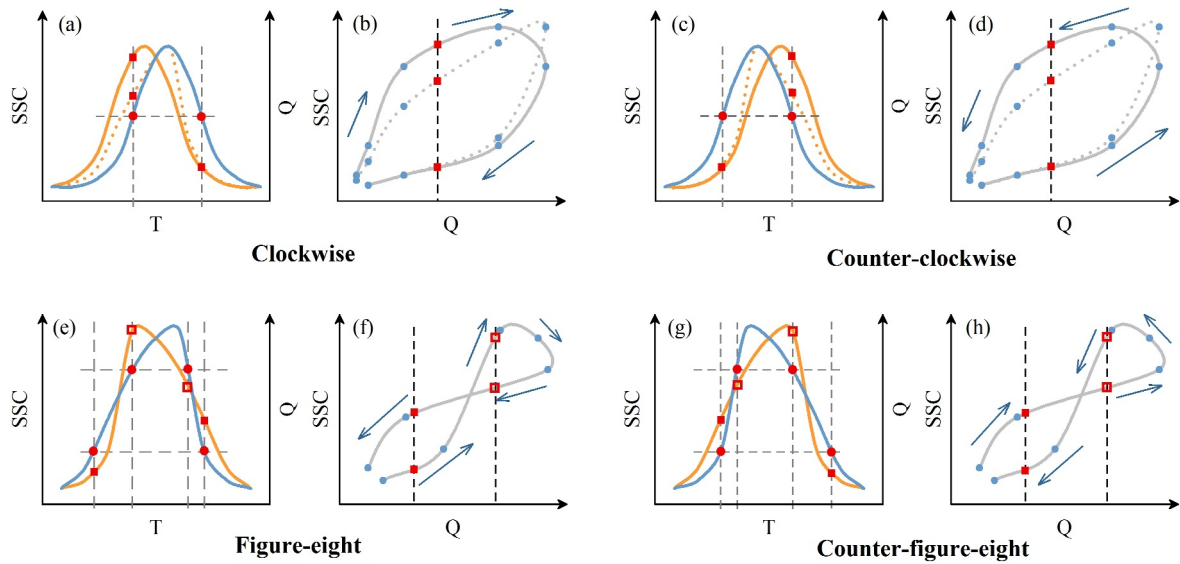


**Figure 1.** Different patterns of hysteresis loops. For each pattern, the left panel shows hydrographs and sediment graphs, while the corresponding hysteresis loop is displayed in the right panel. In the left panel, the Q is represented by the blue line; the solid orange line depicts the SSC peaking asynchronously with Q; the orange dotted line in the clockwise and counter-clockwise loops signifies SSC peaking synchronously with Q. Red dots indicate the same Q, while red squares denote the SSC at the same Q.

hydrological events (Richards, 1984; Walling, 1977). Early studies categorized hysteresis as clockwise or counter-clockwise, depending on whether the SSC peak preceded or followed the Q peak (Burt et al., 1983; Klein, 1984). As the understanding of flood dynamic grew, more complex hysteresis patterns emerged. In 1989, Williams first classified hysteresis loops into five types systematically: single-line, clockwise, counter-clockwise, single-line with hysteresis, and figure-eight (Williams, 1989). Since then, numerous variations have been identified, expanding the understanding of sediment transport during floods. Today, four main patterns dominate hydrological studies: clockwise, counter-clockwise, figure-eight, and complex (Figure 1).

Clockwise hysteresis occurs when the sediment graph rises and falls faster than the hydrograph, creating a loop where SSC peaks before Q. On the graph, SSC decreases sharply during the falling limb, even when discharge remains high (Buendia et al., 2016; Gellis, 2013; Pulley et al., 2019; Varvani et al., 2019). In contrast, counter-clockwise hysteresis occurs when Q peaks before SSC, with SSC lagging during the recession of the hydrograph, producing a flatter loop on the falling limb (Burt et al., 2015; Millares & Monino, 2020; Yeshaneh et al., 2014). The figure-eight hysteresis results from multiple peaks in SSC and Q during a flood, combining clockwise and counter-clockwise loops. It can be categorized into two types: a figure-eight with counter-clockwise loops at low discharge and clockwise loops at high discharge, and a reverse figure-eight with the opposite pattern (Hu et al., 2019; Ram & Terry, 2016; Ranjan & Roshni, 2024; Ziegler et al., 2014). These loops reflect the complex interactions between sediment availability and transport, as SSC and Q cross paths to form the characteristic “8” shape (Lopez-Tarazon et al., 2009; Richards & Moore, 2003; Shojaezadeh et al., 2022; Tananaev, 2012). Complex hysteresis, characterized by multiple SSC and Q peaks, arises from a combination of different hysteresis patterns, often seen during consecutive or prolonged storms (Pulley et al., 2019; Upadhayay et al., 2021; Yibeltal et al., 2023). Irregular precipitation patterns and diverse sediment sources contribute to its non-repetitive shape. Due to its variability and complexity, this pattern is less frequently studied and remains poorly understood.

### 2.3. Quantitative Analysis of Hysteresis Loops

To enhance the analysis of hysteresis mechanisms, researchers developed quantitative indices to address the limitations of graphical hysteresis loops. While visual comparisons offer valuable insights into sediment transport (Asselman, 1999; Williams, 1989), they are insufficient for comparing hydrological and sediment processes across different hydrological events and watersheds (Lawler et al., 2006). In response, indices such as the hysteresis index (HI) and flushing index (FI) were introduced to quantify the direction, magnitude, and sediment mobilization processes (Heathwaite & Bierozza, 2021).

Langlois et al. (2005) first proposed the proportional HI, using logarithmic and exponential fits to Q and SSC data from the rising and falling limbs of the hydrograph. The index quantifies the area ratio between the fitted curves, providing insights into both direction and magnitude. However, it requires extensive data for reliable curve fitting and is sensitive to outliers, making it more suited to simple, clockwise, or counter-clockwise loops.

To simplify the calculation, Lawler et al. (2006) introduced the median discharge HI, which focuses on SSC at the midpoint of discharge ( $Q_{mid}$ ). This method avoids noisy data at the onset and end of the event but is sensitive to event magnitude, limiting its reliability for comparing events of different scales. It also struggles with figure-eight and complex patterns.

Aich et al. (2014) addressed event magnitude variability by proposing a normalized HI, which standardizes Q and SSC to enable direct comparisons across events and watersheds. This index is especially useful for capturing the “first flush” effect and provides separate calculations for the rising and falling limbs. However, its complexity and limitations with figure-eight loops restrict broader applications.

Lloyd et al. (2016a) refined these approaches with the differential HI, which divides discharge into intervals and calculates the average SSC difference between the rising and falling limbs for each interval. This method is well-suited to complex patterns, including multi-peak and figure-eight loops, providing greater accuracy by considering more data points across the hydrograph.

The Flushing Index (FI), introduced by Vaughan et al. (2017), compares sediment concentrations at the beginning of an event and at peak discharge, distinguishing between source- and transport-limited sediment mobilization. Combined with HI, FI offers a more comprehensive analysis of hydrological dynamics and SSC-Q relationships during hydrological events.

These quantitative indices aim to automatically detect hysteresis direction and magnitude (Misset et al., 2019). They enhance the capacity to analyze complex patterns, facilitating comparisons across diverse events and watersheds (Wang et al., 2022). The HI developed by Lloyd et al. (2016a) and the FI by Vaughan et al. (2017) are widely adopted for investigating flood hydrodynamics (Lannergard et al., 2021; Pickering & Ford, 2021; Vale & Dymond, 2020; Wang et al., 2022; Zuecco et al., 2016). In practice, selecting the appropriate index depends on the complexity of observed patterns and data availability. For simpler, unidirectional loops, the proportional HI or median discharge HI offers quick insights. For complex, multi-peak, or figure-eight patterns, the differential HI provides a more robust analysis. In cases of intense sediment mobilization, where sediment is either source- or transport-limited, the FI is most appropriate. These indices enable not only event comparison but also provide critical tools for understanding the mechanisms underlying different hysteresis patterns (Table 1). It should be noted that these indices are based on idealized hysteresis loops, and actual sediment dynamic in hydrological events may exhibit more complex variations due to factors such as rainfall intensity, watershed characteristics, and sediment availability.

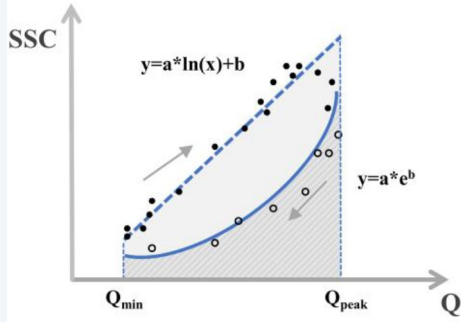
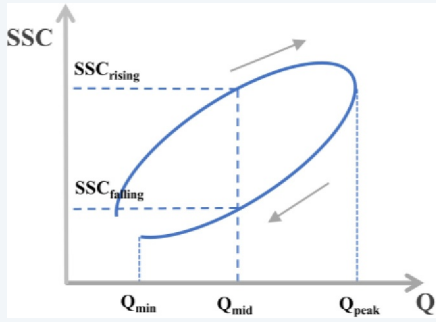
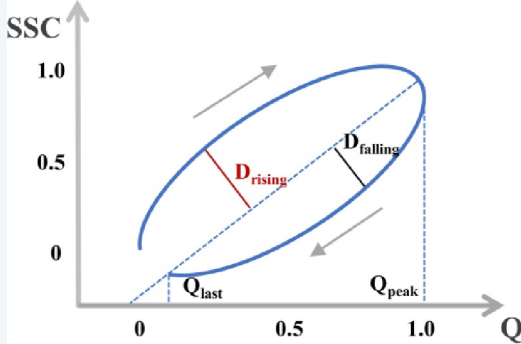
### 3. Global Spatiotemporal Distribution of Hysteresis Research

Hysteresis analysis has become a crucial tool in understanding sediment transport dynamics during hydrological events, with a significant increase in research volume over the past few decades. A total of 514 articles related to event-scale hysteresis analysis in hydrology were identified globally (Text S1 in Supporting Information S2), reflecting the growing importance of this method in studying sediment dynamic.

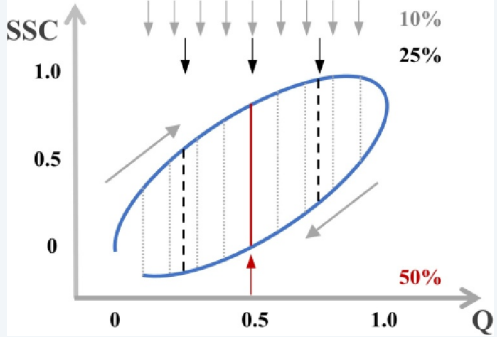
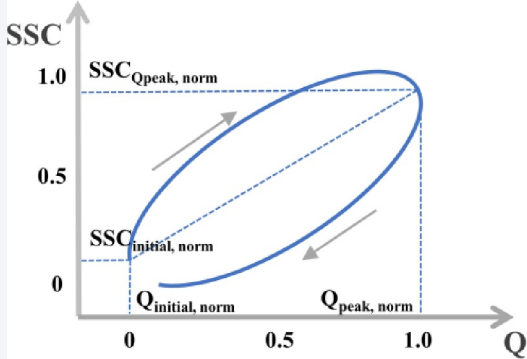
#### 3.1. Temporal Trends in Hysteresis Research

The evolution of hysteresis research can be divided into several key phases, each marked by advancements in both methodology and research focus. Initially, during the 1950s–1970s, researchers primarily relied on sediment rating curves to analyze the relationship between SSC and discharge (Q) (Heidel, 1956; Rendon-Herrero, 1974, 1978; Wood, 1977). However, as studies began to recognize discrepancies between the timing of hydrographs and sediment graphs, the concept of hysteresis emerged. The 1980s saw the development of more systematic studies on hysteresis loops, culminating in the classification of hysteresis patterns, which initiated the qualitative phase of hysteresis analysis (Asselman, 1999; Kelly, 1992; Whiting et al., 1999; Williams, 1989). By 2005, with the introduction of the hysteresis index, hysteresis analysis transitioned to the quantitative phase, allowing for more precise and comparable analyses of sediment transport across different hydrological events and watersheds (Langlois et al., 2005; Lawler et al., 2006).

**Table 1**  
Summary of the Development and Comparison of Quantitative Indices Characterizing Hysteresis Loops

Graphical schematic	Advantages	Limitations	Reference
	<ul style="list-style-type: none"> <li>• Simple and intuitive to quantify both direction and magnitude of hysteresis loops;</li> <li>• Well-suited for identifying basic clockwise and counter-clockwise hysteresis.</li> </ul>	<ul style="list-style-type: none"> <li>• Requires a large amount of data for fitting equations, which makes it vulnerable to outliers;</li> <li>• Difficult to apply to more complex hysteresis patterns like figure-eight loops due to its dependency on fitted curves.</li> </ul>	(Langlois et al., 2005)
$HI = \frac{\int_{Q_{min}}^{Q_{peak}} SSC_{rising} / \int_{Q_{min}}^{Q_{peak}} SSC_{falling}}$	<p><b>Applicable Conditions:</b> Best suited for cases with ample data where separate analysis of the rising and falling limbs of the flood hydrograph is required. Ideal for situations where the temporal dynamics of sediment transport need to be differentiated for each phase of the event.</p> <ul style="list-style-type: none"> <li>• A straightforward approach that avoids noisy data points at the beginning and end of events;</li> <li>• More practical for most applications as it avoids reliance on full-fitting curves.</li> </ul>	<ul style="list-style-type: none"> <li>• Sensitive to event magnitude, meaning that it might underestimate the hysteresis index for high SSC values;</li> <li>• Like Langlois' index, it is unsuitable for complex hysteresis patterns such as figure-eight.</li> </ul>	(Lawler et al., 2006)
	$Q_{mid} = 0.5 * (Q_{peak} - Q_{min}) + Q_{min}$ $HI = \begin{cases} SSC_{rising}/SSC_{falling} - 1 & SSC_{rising} > SSC_{falling} \\ 1 - SSC_{falling}/SSC_{rising} & SSC_{rising} \leq SSC_{falling} \end{cases}$	<p><b>Applicable Conditions:</b> Ideal for situations with limited monitoring data. This index provides reliable results even when data collection is sparse or incomplete, making it suitable for cases where data precision or availability is constrained.</p>	
	<ul style="list-style-type: none"> <li>• Facilitates direct comparison between different events and watersheds due to its normalization of SSC and Q values;</li> <li>• Accounts for the first flush phenomenon, separating the analysis of the rising and falling limbs.</li> </ul>	<ul style="list-style-type: none"> <li>• Despite its strengths, this index remains unsuitable for complex hysteresis patterns like figure-eight;</li> <li>• The calculation can be intricate due to the need for detailed rising and falling limb analysis.</li> </ul>	(Aich et al., 2014)
$Q_{i,norm} = Q_i / Q_{peak}; SSC_{i,norm} = SSC_i / SSC_{peak}$ $HI = D_{rising} + D_{falling}$	<p><b>Applicable Conditions:</b> Suitable for comparing different magnitudes of hydrological events or across various watershed scales. Best used when cross-event or cross-watershed comparison is necessary, providing a robust framework for analyzing variations in sediment dynamics.</p>		

**Table 1**  
Continued

Graphical schematic	Advantages	Limitations	Reference
 <p> <math>Q_{i,norm} = (Q_i - Q_{min}) / (Q_{peak} - Q_{min})</math>  <math>SSC_{i,norm} = (SSC_i - SSC_{min}) / (SSC_{peak} - SSC_{min})</math>  <math>HI = \sum_{i=1}^n (SSC_{i,rising} - SSC_{i,falling}) / n</math> </p>	<ul style="list-style-type: none"> <li>• Suitable for all hysteresis patterns, including complex figure-eight loops.</li> <li>• Provides a more robust analysis by examining multiple sections of the hysteresis loop.</li> </ul>	<ul style="list-style-type: none"> <li>• The complexity of the calculations can be a limitation, requiring a large amount of precise data to achieve accurate results.</li> </ul>	(Lloyd et al., 2016a)
 <p> <math>FI = SSC_{Q_{peak,norm}} - SSC_{initial,norm}</math> </p>	<ul style="list-style-type: none"> <li>• Effectively reflects the sediment mobilization intensity and sediment condition in the watershed;</li> <li>• Works well when combined with other indices, such as the HI, to offer a comprehensive view of sediment transport.</li> </ul>	<ul style="list-style-type: none"> <li>• Primarily designed for more specific cases of flushing or dilution, limiting its general applicability to other types of hysteresis.</li> </ul>	(Vaughan et al., 2017)

*Note.* The hysteresis loops and formulations presented are idealized representations. Actual sediment concentration and discharge dynamics in hydrological events may exhibit more complex variations.

The temporal growth in hysteresis research is depicted in Figure 2, which shows a sharp increase in publications starting in the early 2000s. The rate of publication continued to rise, reflecting the increasing recognition of hysteresis analysis as a vital tool for understanding complex sediment dynamic, particularly in flood-prone regions. The surge in publications from 2020 onwards further underscores the heightened focus on hysteresis analysis in the context of climate change and more frequent extreme weather events. The increasing precision of monitoring technologies and the ability to collect high-frequency data have played a pivotal role in this trend, enabling more detailed studies of multi-peak and complex hysteresis loops.

### 3.2. Spatial Distribution of Hysteresis Research

Spatially, hysteresis research has been concentrated in regions with specific hydrological characteristics, as shown in Figure 3. A major concentration of research, accounting for over 70% of the studies, is found in arid and semi-arid regions and Mediterranean climates, which share similar erosion and sediment transport characteristics. These regions typically have sufficient sediment availability, and sediment mobilization is heavily influenced by episodic rainfall events (Alexandrov et al., 2007; Diaf et al., 2020; Gao et al., 2013; Mihiranga et al., 2021). For

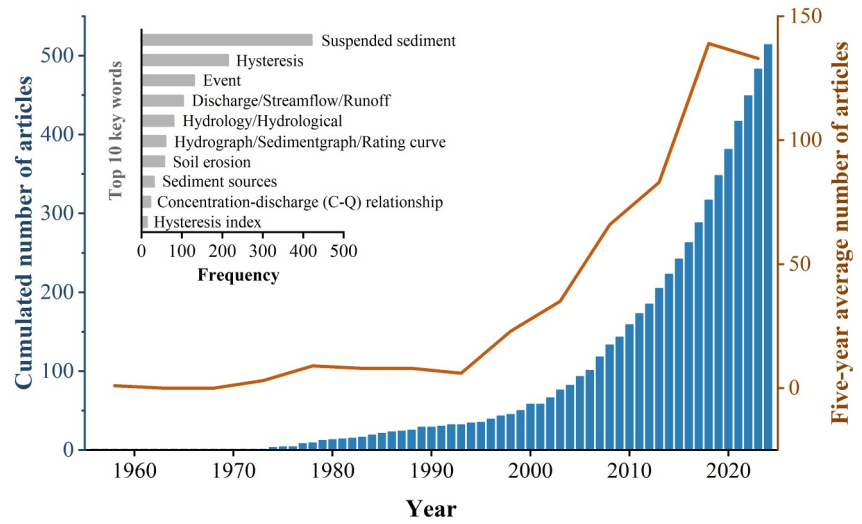


**Figure 2.** Development trends in hysteresis analysis research and distribution of key words (1950s–2020s).

example, in the United States, much of the research has focused on regions where flash floods and intense rainfall events trigger rapid sediment mobilization (Javed et al., 2021; Marin-Ramirez et al., 2024). Similarly, in China, large river systems such as the Yellow River and the Yangtze have been central to studies of sediment dynamics, particularly in response to human activities like dam construction, deforestation, and agricultural practices (Li et al., 2024; Ren et al., 2020; Zhao et al., 2017). Mediterranean regions, such as Spain, Italy, and France, share similar characteristics, where the dynamic shifts in sediment transport during episodic storms are of primary concern. These regions, too, have seen increased research into how droughts followed by heavy rainfall affect sediment dynamics and flood processes (Esteves et al., 2019; Pagano et al., 2019; Tuset et al., 2022).

Beyond these areas, tropical regions have also seen increasing research activity, driven by the growing frequency and intensity of extreme events. In countries like Brazil, Ethiopia, and Malaysia, the frequency of intense rainfall events has been increasing due to climate change, leading to more frequent and severe floods. In Brazil, research has focused on the impact of deforestation and land-use changes on sediment fluxes during floods, highlighting the importance of hysteresis analysis in understanding sediment mobilization in rapidly changing landscapes (de Menezes et al., 2020; Londero et al., 2018). Similarly, in Ethiopia and other parts of Southeast Asia, studies have

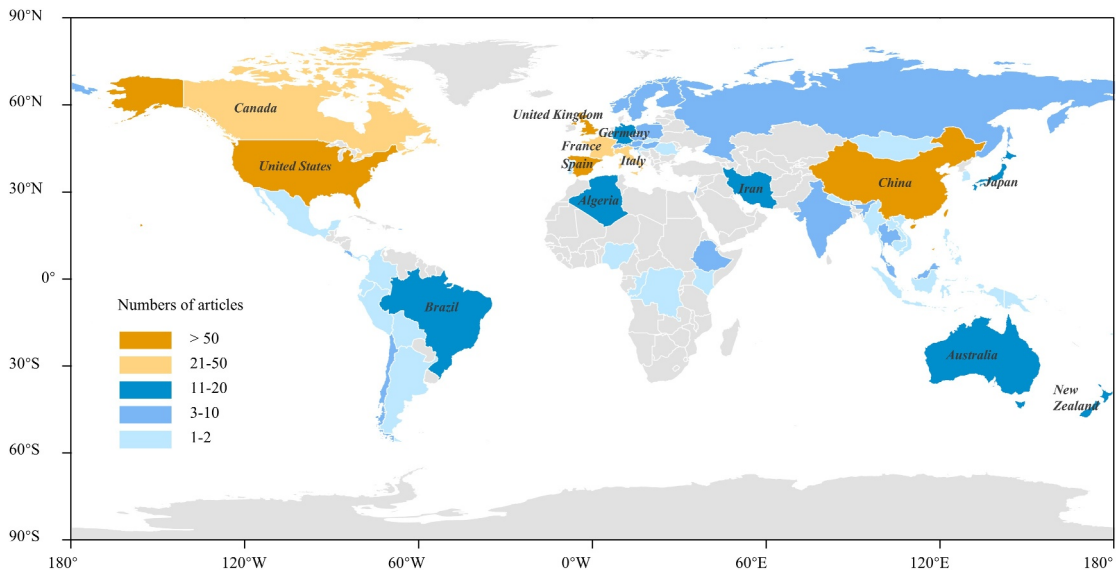


**Figure 3.** Spatial distribution of hysteresis research globally.



explored the effects of rainfall variability and land-use changes on sediment transport during hydrological events, further underlining the role of hysteresis analysis in capturing complex sediment dynamics in tropical regions (Dominic et al., 2015; Yeshaneh et al., 2014; Yibeltal et al., 2023). Additionally, high-altitude regions such as the Alps, Himalayas, and Andes are increasingly becoming focal points for hysteresis research. These areas, which experience snowmelt-driven runoff and freeze-thaw cycles, display unique hysteresis patterns that differ from those found in lower-altitude regions. Snowmelt and ice dynamics are particularly important factors influencing sediment transport in these regions, and hysteresis patterns often reflect delayed sediment transport and complex interactions between water and sediment (Carrillo & Mao, 2020; Engel et al., 2024; Manseau et al., 2022; Swift et al., 2021). The growing frequency of extreme hydrological events in these high-altitude regions, also exacerbated by climate change, has led to increased interest in understanding the dynamics of sediment mobilization, particularly in snowmelt-driven events. As these areas experience more frequent hydrological events due to climate change, hysteresis analysis becomes increasingly critical for understanding sediment dynamics in these vulnerable regions.

#### 4. Applications of Hysteresis Analysis in Hydrological Research

Hysteresis analysis has become an essential tool in the hydrological study of hydrological events, serving not only as a method for classifying different flood types but also as a means of characterizing the distinct features of these events (Valente et al., 2021; Zou et al., 2022). By categorizing floods based on hysteresis patterns, researchers can gain deeper insights into the environmental factors shaping these patterns and evaluate the sediment transport capacity of each flood type (Rustomji et al., 2008). This approach enables the identification of key hydrological events and their underlying mechanisms, offering valuable information for effective watershed and river management.

##### 4.1. Characterization and Classification of Hydrological Events

Hydrological events are complex hydrological processes influenced by a combination of meteorological and geomorphological factors. Effectively characterizing and classifying these events is essential for understanding sediment transport dynamic and developing sustainable watershed management strategies (Pietron et al., 2015; Ranjan & Roshni, 2024). Characterization focuses on quantifying both pre-event conditions and hydrological responses during the event, while classification groups hydrological events based on shared characteristics, offering deeper insights into the mechanisms driving sediment transport.

Accurate hydrological event characterization involves assessing pre-event conditions and event magnitude through a set of hydrological, meteorological, and sediment-related variables (Table 2). As outlined in Table 2, these variables capture both the antecedent conditions and the overall dynamic. Precipitation variables such as total precipitation (P), precipitation intensity (PI), maximum 30-min intensity (I30), and accumulated precipitation over 1, 5, and 10 days before the event (AP1, AP5, AP10) describe the meteorological factors that set the stage for the flood. Coupled with baseflow ( $Q_b$ ), these indicators help assess the watershed moisture state, which is crucial for understanding how it responds to subsequent rainfall (Baker & Showers, 2019; Oeurng et al., 2010). Hydrological variables—including runoff depth (H), runoff coefficient ( $R_c$ ), mean discharge (Q), peak discharge ( $Q_{peak}$ ), and event duration (T), along with the durations of the rising ( $T_r$ ) and falling ( $T_f$ ) limbs—capture the flow characteristics during the flood. These factors reveal the intensity, duration, and variability of the hydrological event (Nadal-Romero et al., 2008; Oeurng et al., 2011). Sediment properties such as total sediment yield (SSY), mean SSC, and peak SSC ( $SSC_{peak}$ ) provide insights into the amount and timing of sediment transport (Pagano et al., 2019; Tian et al., 2016).

The introduction of quantitative hysteresis indices, such as the hysteresis index (HI) and flushing index (FI), has enhanced the ability to characterize hydrological events. These indices capture the nonlinear interactions between SSC and Q, adding depth to traditional metrics by reflecting how sediment transport changes during the different phases of a flood (Heathwaite & Bieroza, 2021; Hu et al., 2019; Liu et al., 2021; Millares & Monino, 2020). This comprehensive set of variables, when considered together, offers a robust framework for describing hydrological events and their sediment dynamics.

Traditionally, flood classification has relied on hydrological and meteorological variables to group events with similar characteristics, often using clustering techniques to analyze patterns in flood behavior (Jansson, 2002; Lyu et al., 2020; Oeurng et al., 2011; Pagano et al., 2019). This approach provides a general understanding of flood

**Table 2**  
*Variables Used to Characterize Hydrological Events*

	Variables	Abbreviation	Explanation
Precipitation properties	Precipitation (mm)	$P$	Total precipitation
	Precipitation intensity ( $\text{mm h}^{-1}$ )	$PI$	Precipitation intensity
	Precipitation intensity in 30 min ( $\text{mm h}^{-1}$ )	$I_{30}$	Maximum 30 min precipitation intensity
	Antecedent 1 day precipitation (mm)	$API$	Accumulated precipitation of 1 day prior to the event
	Antecedent 5 days precipitation (mm)	$AP5$	Accumulated precipitation of 5 days prior to the event
	Antecedent 10 days precipitation (mm)	$API0$	Accumulated precipitation of 10 days prior to the event
Hydrology properties	Baseflow ( $\text{m}^3 \text{s}^{-1}$ )	$Q_b$	Baseline discharge between two different event
	Runoff depth (mm)	$H$	The ratio between total runoff and watershed area
	Runoff coefficient (%)	$Rc$	The ratio between runoff depth and total precipitation
	Discharge ( $\text{m}^3 \text{s}^{-1}$ )	$Q$	Mean discharge
	Peak discharge ( $\text{m}^3 \text{s}^{-1}$ )	$Q_{peak}$	Maximum discharge
	Duration (h)	$T$	Duration of the whole event
	Duration of rising limb (h)	$T_r$	Duration of the event rising stage
	Duration of falling limb (h)	$T_f$	Duration of the event recession stage
Sediment properties	Sediment yield ( $\text{t km}^{-2}$ )	$SSY$	Total sediment load
	Suspended sediment concentration ( $\text{kg m}^{-3}$ )	$SSC$	Mean suspended sediment concentration
	Peak suspended sediment concentration ( $\text{kg m}^{-3}$ )	$SSC_{peak}$	Maximum suspended sediment concentration

magnitude and hydrological responses. However, the incorporation of hysteresis analysis has expanded the scope of classification by adding sediment dynamics into the mix. Hysteresis patterns—clockwise, counterclockwise, figure-eight, and complex loops—provide key insights into the timing and source of sediment transport during hydrological events (Duvert et al., 2010; Esteves et al., 2019; Gao et al., 2018). These patterns can distinguish between floods where sediment is mobilized early (clockwise) or late (counter-clockwise) in the event, revealing important differences in sediment transport mechanisms (Cao et al., 2021; Oeurng et al., 2010). As a result, hysteresis analysis allows for a more refined classification of floods based on the relationship between SSC and  $Q$ .

In recent years, the integration of traditional flood classification methods with hysteresis analysis has led to a more holistic approach to understanding flood dynamics. By combining conventional metrics with hysteresis insights, researchers can better identify the drivers of different sediment transport behaviors. Furthermore, advances in machine learning and artificial intelligence, such as artificial neural networks, have allowed for even more precise classification by capturing finer details in the hydrographs of water and sediment (Hamshaw et al., 2018). These developments have expanded the ability to classify hydrological events beyond the four primary hysteresis patterns, providing a more nuanced understanding of flood processes.

#### 4.2. Revelation of Sediment Sources and Transport Processes

Various hydrometeorological factors, along with watershed characteristics and human activities, play critical roles in shaping hydrological events and their hydrological processes (Fortesa et al., 2020; Wenng et al., 2021; Zhao et al., 2017). Suspended sediment (SS) dynamics during hydrological events can be broadly categorized into sediment sources and transportation processes before reaching the watershed outlet. These stages are influenced by factors that regulate sediment availability and hydrological connectivity, leading to different hysteresis patterns (Figure S1) (Cheraghi et al., 2016; Lannergard et al., 2021; Vercruyssen & Grabowski, 2019). In this study, we classify and analyze the potential factors affecting hysteresis, focusing on hydrometeorological conditions, watershed properties, and human activities. A detailed list of references for each influencing factor is provided in Table 3.

**Table 3**  
*Influencing Factors of Hysteresis Patterns and References*

Influencing factors		Influencing type	Mechanisms	References
Hydrometeorological factors	Precipitation distribution	Positive/Negative	<ul style="list-style-type: none"> <li>Localized precipitation near the basin outlet quickly mobilizes proximal sediment, leading to clockwise hysteresis;</li> <li>Widespread rainfall across the basin activates multiple distant sediment sources, delaying transport and creating counter-clockwise or complex hysteresis patterns.</li> </ul>	Al Sawaf et al. (2024), Fortesa et al. (2021), Rose and Karwan (2021), Fang (2019), Ziegler et al. (2014)
	Precipitation magnitude	Positive	<ul style="list-style-type: none"> <li>High-intensity rainfall generates immediate runoff, rapidly mobilizing nearby sediment, causing clockwise hysteresis;</li> <li>Larger storms can transport sediment from upstream areas, resulting in delayed sediment peaks and counter-clockwise or figure-eight hysteresis.</li> </ul>	Yu et al. (2023), Zhu et al. (2023), Haddadchi and Hicks (2021), Vale and Dymond (2020), Wymore et al. (2019), Ares et al. (2016), Perks et al. (2015), Ziegler et al. (2014), Fang et al. (2011), Oeurng et al. (2011), Rodriguez-Blanco et al. (2010), Mano et al. (2009), Sadeghi et al. (2008a, 2008b), Alexandrov et al. (2007), Rovira and Batalla (2006), Sammori et al. (2004), Goodwin et al. (2003), Jeje et al. (1991)
	Antecedent moisture	Positive	<ul style="list-style-type: none"> <li>High antecedent soil moisture reduces infiltration, increasing surface runoff and accelerating sediment transport, leading to quick sediment responses and clockwise hysteresis;</li> <li>Drier conditions increase soil absorption, slowing sediment movement, resulting in counter-clockwise hysteresis as sediment lags behind discharge.</li> </ul>	Rose and Karwan (2021), Vale and Dymond (2020), Bierzoza and Heathwaite (2015), Dominic et al. (2015), Gimenez et al. (2012), Soler et al. (2008), Langlois et al. (2005)
	Events timing	Positive/Negative	<ul style="list-style-type: none"> <li>Early wet season storms flush accumulated sediment from dry channels, leading to strong clockwise hysteresis;</li> <li>Later in the season, sediment depletion can result in counter-clockwise hysteresis, especially if only distant sources are mobilized.</li> </ul>	Alavez-Vargas et al. (2021), Lannergard et al. (2021), Buendia et al. (2016), Perks et al. (2015), Dominic et al. (2015), Tananaev (2015), Fan et al. (2013), Megnounif et al. (2013), Gao and Josefson (2012), Fang et al. (2008), Rovira and Batalla (2006)
	Events sequence	Negative	<ul style="list-style-type: none"> <li>Small initial events deposit sediment in channels, increasing sediment availability for subsequent floods, leading to clockwise hysteresis;</li> <li>Large events deplete sediment, reducing the transport capacity in later events and leading to weaker or counter-clockwise hysteresis.</li> </ul>	Xue et al. (2024), Martin et al. (2014), Wilson et al. (2012), Rodriguez-Blanco et al. (2010), Smith and Dragovich (2009), Baca (2008), Rovira and Batalla (2006)
Watershed properties	Topography	Positive	<ul style="list-style-type: none"> <li>Steep slopes accelerate runoff and sediment movement, promoting clockwise hysteresis as sediment is quickly mobilized and transported downstream;</li> </ul>	Xiao et al. (2024), Keesstra et al. (2019), Pagano et al. (2019)

**Table 3**  
*Continued*

Influencing factors	Influencing type	Mechanisms	References	
Soil properties	Negative	<ul style="list-style-type: none"> <li>• Flat terrain slows sediment transport, leading to delayed sediment peaks and counter-clockwise hysteresis.</li> <li>• Coarse-grained soils (e.g., sandy soils) allow high infiltration, reducing runoff and sediment detachment, resulting in weaker hysteresis or linear SSC-Q relationships;.</li> <li>• Fine-grained soils (e.g., clay) increase surface runoff and sediment transport, contributing to stronger clockwise hysteresis during intense rainfall events</li> </ul>	Long et al. (2024), Fortesa et al. (2021), Cheraghi et al. (2016), Hudson (2003)	
Basin size	Negative	<ul style="list-style-type: none"> <li>• Small basins have shorter sediment transport distances, allowing quick sediment mobilization and transport, often leading to clockwise hysteresis;</li> <li>• Large basins have longer transport distances, delaying sediment peaks and leading to counter-clockwise hysteresis. Larger basins may also produce figure-eight hysteresis due to multiple tributaries and variable sediment sources.</li> </ul>	Bolade and Hansen (2023), Wang et al. (2022), Fortesa et al. (2021), Tena et al. (2014), Fang et al. (2011), Jansson (2002), Steegen et al. (2000), Heidel (1956)	
Human activities	Land-use	Positive/Negative	<ul style="list-style-type: none"> <li>• Urbanized areas and agricultural practices create impermeable surfaces and increase sediment connectivity, leading to rapid sediment transport and clockwise hysteresis during hydrological events;</li> <li>• Forested and vegetated areas slow sediment movement by intercepting runoff and reducing sediment availability, resulting in delayed sediment transport and counter-clockwise hysteresis, especially during high-magnitude events.</li> </ul>	Safdar et al. (2024), Yu et al. (2023), Zhou et al. (2023), Haddadchi and Hicks (2021), Zarnaghsh and Husic (2021), Chen and Chang (2019), Hu et al. (2019), Bender et al. (2018), Liu et al. (2017), Yeshaneh et al. (2014), Gellis (2013), Hughes et al. (2012), Lenzi and Marchi (2000)
	Dam and reservoir construction	Negative	<ul style="list-style-type: none"> <li>• Dams and reservoirs trap sediment upstream, delaying its transport downstream and causing counter-clockwise hysteresis as sediment peaks occur after discharge peaks;</li> <li>• Regulated water and sediment flows from reservoirs alter natural sediment transport processes, potentially creating complex or figure-eight hysteresis patterns. Seasonal regulation can reverse normal sediment timing and transport.</li> </ul>	Ghosh and Munoz-Arriola (2023), Lyu et al. (2020), Ren et al. (2020), Huang et al. (2018), Tena et al. (2014), Fan et al. (2013)

#### 4.2.1. Hydrometeorological Factors

Hydrometeorological factors, particularly precipitation intensity, distribution, event timing, and sequence, are key drivers of hysteresis patterns. Precipitation is the primary force controlling soil erosion and sediment transport during hydrological events. It directly influences the availability of sediment and the hydrological connectivity within a watershed.

Intense rainfall events result in the rapid mobilization of sediment, leading to clockwise hysteresis patterns, where the peak SSC precedes the peak discharge (Q) (Jansson, 2002). This pattern typically reflects the quick response of nearby sediment sources, often located close to the river channel (Geeraert et al., 2015; Hudson, 2003; Strauch et al., 2018). For example, during small magnitude hydrological events, the sediment is often mobilized from proximal sources such as riverbanks, contributing to a swift sediment response (El Azzi et al., 2016; Perks et al., 2015; Rose & Karwan, 2021). Conversely, during larger hydrological events, when precipitation intensity is higher and more widespread, distant sediment sources are mobilized, resulting in counter-clockwise hysteresis (Garcia-Comendador et al., 2021; Lefrancois et al., 2007). In such cases, the sediment lag is due to the time required to transport eroded material from upstream or distant parts of the watershed (Fortesa et al., 2021; Oeurng et al., 2011). The occurrence of counter-clockwise hysteresis in larger events is also linked to processes such as bank collapse, which tends to occur during the falling limb of the hydrograph when stream power decreases (Lannergard et al., 2021).

Precipitation distribution also plays a significant role in hysteresis patterns. When localized precipitation occurs near the watershed outlet, sediment from nearby sources is mobilized quickly, producing clockwise hysteresis even in small events (Huang et al., 2018; Sadeghi et al., 2017). In contrast, when the precipitation center is farther upstream, sediment from distant sources is mobilized, which often leads to counter-clockwise hysteresis as the sediment takes longer to reach the outlet (Doomen et al., 2008; Fang, 2019; Hu et al., 2019). Widespread precipitation across a watershed, especially during high-intensity storms, can activate multiple sediment sources simultaneously, giving rise to complex or figure-eight hysteresis patterns, as these events involve both near and distant sources of sediment (Rose & Karwan, 2021).

The timing and sequence of hydrological events are additional factors that influence sediment transport. At the onset of the wet season, when large amounts of sediment have accumulated during the dry period, early hydrological events tend to flush this material into the river channels, producing strong clockwise hysteresis (Alavez-Vargas et al., 2021; Duvert et al., 2010; Gray et al., 2014). As the wet season progresses and sediment becomes depleted, subsequent hydrological events may begin to draw from more distant sources, resulting in counter-clockwise hysteresis (Coch et al., 2018; Salant et al., 2008; Zou et al., 2022). Additionally, the sequence of hydrological events impacts the availability of sediment: smaller events can lead to sediment accumulation, increasing the availability of sediment for larger, subsequent events. On the other hand, larger initial floods can deplete sediment stores, leading to lower sediment concentrations in later events, despite higher discharge, and producing more complex hysteresis patterns (Figure S2) (Martin et al., 2014; Rovira & Batalla, 2006).

#### 4.2.2. Watershed Properties

Watershed characteristics, including topography, soil properties, and watershed size, play critical roles in shaping the transport paths of sediment and the hysteresis patterns that result during hydrological events. These properties govern how quickly and efficiently sediment is mobilized and transported from different parts of the watershed to the river channel.

Topography is one of the most important factors influencing sediment transport. Steeper slopes increase surface runoff and enhance the energy available to mobilize sediment, leading to more rapid transport and clockwise hysteresis (Li et al., 2019; Richards & Moore, 2003). In contrast, flatter terrain slows sediment transport, often resulting in counter-clockwise hysteresis as sediment peaks lag behind discharge peaks (Garcia-Comendador et al., 2021; Sun et al., 2024). In watersheds with high drainage density, hydrological connectivity is stronger, which facilitates the continuous transport of sediment throughout the hydrological event, often prolonging the falling limb and contributing to counter-clockwise hysteresis (Cao et al., 2021; Sherriff et al., 2016). In regions with complex topography, the timing and magnitude of sediment transport can vary widely, leading to more intricate hysteresis patterns, such as figure-eight loops (Misset et al., 2019).

Soil properties are another key determinant of sediment availability and transport. Coarse-grained soils, which promote infiltration, often reduce the amount of surface runoff and the detachment of sediment, resulting in weaker hysteresis effects or even linear SSC-Q relationships (Bettel et al., 2022; Fang et al., 2015; Sadeghi et al., 2018). In contrast, fine-grained soils, such as clay and silt, tend to increase surface runoff and sediment detachment, leading to more pronounced clockwise hysteresis patterns (Juez et al., 2018; Landers & Sturm, 2013; Serra et al., 2022; Upadhayay et al., 2021). The heterogeneity of soil particle sizes within a watershed can further

influence hysteresis patterns, with finer particles being more readily transported over longer distances, resulting in a delayed sediment response during larger hydrological events (Cheraghi et al., 2016; Pulley et al., 2019).

The size of the watershed also plays a crucial role in determining sediment transport dynamics. In smaller watersheds, sediment sources are located closer to the river outlet, leading to rapid sediment mobilization and transport, often resulting in clockwise hysteresis (Heidel, 1956). Larger watersheds, however, encompass more complex tributary networks and have longer sediment transport distances, resulting in delayed sediment delivery and counter-clockwise hysteresis patterns as sediment from distant sources reaches the river channel after the discharge peak (Blothe & Hoffmann, 2022; Oeurng et al., 2010). In some cases, large watersheds can exhibit figure-eight hysteresis patterns, particularly when multiple sediment sources are activated at different stages of the hydrological event (Tena et al., 2014).

#### 4.2.3. Human Activities

Human activities, such as land-use changes, vegetation cover, and the construction of dams and reservoirs, significantly alter the natural sediment transport processes in a watershed. These activities modify both the availability of sediment and the pathways through which it is transported, leading to changes in hysteresis patterns.

Land-use practices, such as agriculture and urbanization, increase sediment availability and connectivity by reducing vegetation cover and increasing impermeable surfaces. This often results in faster sediment mobilization and clockwise hysteresis during hydrological events (Ram & Terry, 2016; Safdar et al., 2024; Zarnaghsh & Husic, 2021). Agricultural practices, such as tillage, can loosen soil, making it more susceptible to erosion and transport, while urban areas, with their extensive drainage networks, enhance connectivity between sediment sources and the river channel, further accelerating sediment transport (Haddadchi & Hicks, 2021; Singh et al., 2020). Conversely, areas with high vegetation cover, such as forests or restored ecosystems, tend to stabilize soil, reducing sediment detachment and leading to delayed sediment peaks and counter-clockwise hysteresis during larger hydrological events (Valente et al., 2021; Zhou et al., 2023). In these cases, sediment is often trapped by vegetation during smaller events, while larger floods may mobilize sediment from more distant sources.

The construction of dams and reservoirs has a particularly strong impact on sediment transport. These structures trap sediment upstream, disrupting the natural sediment flux and often producing counter-clockwise hysteresis as sediment transport lags behind discharge (Geeraert et al., 2015; Singh et al., 2020; Tolorza et al., 2014). Reservoir operations, particularly the timing of water releases, can further complicate sediment dynamics, leading to more complex hysteresis patterns depending on how sediment is managed. Seasonal flow regulation can also reverse the natural timing of sediment transport, with sediment being transported during periods of low natural flow, altering the overall hydrological response of the watershed (Ren et al., 2020; Soler et al., 2008). This dynamic is highlighted in Figure S2, which shows how reservoir construction alters sediment transport processes.

These human activities not only affect sediment availability and transport but also influence the broader hydrological and sediment connectivity of the watershed. By analyzing the impacts of land-use and dam construction on hysteresis patterns, researchers can better understand the role of human interventions in shaping sediment dynamics during hydrological events.

The interplay between hydrometeorological conditions, watershed properties, and human activities forms a complex network influencing sediment transport and hysteresis during hydrological events. These factors rarely act in isolation, instead interacting synergistically or competitively to shape sediment responses (Heathwaite & Bieroza, 2021; Stubblefield et al., 2007; Tsyplenkov et al., 2020; Ziegler et al., 2014). Identifying the primary drivers of these processes is critical for effective watershed management. Recent advances in hydrological research have employed techniques such as Principal Component Analysis, Partial Least Squares-Structural Equation Modeling, and machine learning to disentangle dominant factors influencing hydrological events in specific watersheds (Yu et al., 2023; Zarnaghsh & Husic, 2021). These approaches not only deepen our understanding of the interactions between natural and anthropogenic forces but also provide actionable insights for optimizing watershed management and mitigating the impacts of extreme hydrological events.

### 4.3. Evaluation of Different Hysteresis Patterns

Building on the classification of hydrological events and identification of key influencing factors, numerous studies have examined the relationship between hysteresis patterns and their respective contributions to total sediment yield. This analysis highlights the most erosion-prone flood types and their associated sediment transport processes, providing valuable insights for river watershed management.

Within a specific watershed, the distribution of hysteresis patterns and their sediment yield contributions often vary significantly over time, revealing distinct sediment transport characteristics for each pattern (Bieroza & Heathwaite, 2015; Esteves et al., 2019; Nadal-Romero et al., 2008). For example, while clockwise hysteresis is frequently observed, its contribution to total sediment yield is typically small. In contrast, complex and figure-eight patterns, though less common, tend to yield higher sediment loads due to their longer duration and higher sediment transport capacity from multiple peak events (Dominic et al., 2015; Megnounif et al., 2013; Tsyplenkov et al., 2020).

Counter-clockwise hysteresis events often result in greater sediment transport compared to clockwise events under similar discharge conditions (Lannergard et al., 2021). A study in a Russian mountainous watershed found that nearly 50% of the total sediment yield was transported by just 10% of counter-clockwise events (Tsyplenkov et al., 2020). Similarly, Haddadchi and Hicks (2021) demonstrated that while counter-clockwise events comprised 40% of all events, they accounted for over 90% of sediment transport. This discrepancy is likely due to the ability of counter-clockwise events, driven by intense rainfall, to mobilize sediment from distant sources within the watershed. During these events, sediment delivery lags behind river discharge, with continued sediment supply during the falling limb of the hydrograph, unlike clockwise events.

Counter-clockwise and complex hysteresis patterns are generally considered the most efficient for sediment transport (Esteves et al., 2019), primarily due to their ability to sustain sediment delivery over longer periods, particularly in large-scale hydrological events. Therefore, assessing hysteresis patterns based solely on frequency is insufficient. A more informative approach evaluates each pattern's contribution to total sediment load, which is essential for identifying high-risk hydrological events and prioritizing management efforts.

By analyzing these contributions and understanding which flood types dominate sediment transport, researchers and water resource managers can better predict which hydrological events are most likely to cause significant erosion and sediment deposition, allowing for more targeted and effective watershed management strategies.

## 5. Limitations and Prospects

The hysteresis method has been instrumental in revealing sediment responses to highly variable discharge during hydrological events, yielding valuable insights into sediment transport dynamics. However, several key challenges remain, particularly in the collection of high-resolution data. Continuous and simultaneous monitoring of suspended sediment concentration (SSC) and discharge ( $Q$ ) is critical for accurately capturing the temporal evolution of sediment transport processes. The absence of reliable, real-time data, especially during high-flow conditions, limits the ability to develop robust models and conduct thorough hysteresis analyses. Current data collection practices, often intermittent and event-specific, fall short of representing the full variability and complexity of sediment transport. This presents a significant technical challenge, impeding researchers' capacity to assess sediment transport across different hydrological events and watersheds.

In addition to this technical barrier, two primary research gaps persist that hinder the broader application of hysteresis methods. In the following sections, we discuss these challenges and propose prospective directions to address them, focusing on both methodological advancements and practical implementation strategies.

### 5.1. Optimized Hysteresis Index (HI) for Various Hysteresis Patterns

The existing hysteresis indices commonly exhibit notable limitations, such as restricted applicability to events of varying magnitudes and difficulties in quantifying complicated hysteresis patterns. These issues were addressed by normalizing the observed values of  $Q$  and SSC and dividing  $Q$  into multiple intervals. The hysteresis index for each  $Q$  interval was individually calculated and then averaged to derive the final hysteresis index (HI). This methodology not only improved result accuracy but also demonstrated versatility across diverse hysteresis

patterns, making it the most widely employed HI presently. However, our literature review suggests that its optimal performance is predominantly observed when applied to simple uni-directional hysteresis patterns (clockwise and counter-clockwise).

On the one hand, calculating  $Q$  at specific intervals adds complexity to the computation process. Lloyd et al. (2016a) proposed that enhancing precision in results is achievable by increasing the number of  $Q$  intervals. Dividing  $Q$  into 10% intervals is suitable for 95% of events, and 5% intervals cover 100% of events, although this necessitates a substantial amount of measured data. Moreover, for figure-eight and complex hysteresis patterns, instances of elevated and diminished SSC during the rising limb compared to the falling limb are observed across various intervals along the entire hydrograph. This leads to the possibility of obtaining HI values that can be either positive or negative, contingent upon the duration during which the rising limb's SSC is higher or lower than that of the falling limb. In practical applications, to distinguish these patterns from clockwise hysteresis (positive value), counter-clockwise hysteresis (negative value), and no hysteresis (zero value), a detailed examination is required to assess whether both positive and negative hysteresis indices simultaneously occur within the selected time intervals. This process is crucial for ultimately determining the specific hysteresis pattern.

On the other hand, the essence of HI encompasses two crucial aspects: the sign (indicating the hysteresis loop direction) and the magnitude (representing the hysteresis extent). A positive value denotes clockwise hysteresis, while a negative value indicates counter-clockwise hysteresis. A larger absolute value implies a more pronounced hysteresis effect, signifying a greater difference in SSC between the rising and falling limbs under the same  $Q$ . As a result, quantified HI is often employed in attribution analysis to explore its correlation with influencing factors. However, empirical studies have shown that correlations between influencing factors and HI tend to degrade when figure-eight and complex hysteresis patterns constitute a significant proportion. This degradation is attributed to significant variability in SSC in the rising and falling limbs for both of these hysteresis patterns. The average HI, calculated based on multiple  $Q$  intervals, does not adequately capture their dynamic variations. When analyzing the correlation with influencing factors, distinguishing between complex hysteresis patterns (figure-eight, complex) and simple hysteresis patterns (clockwise, counter-clockwise) becomes challenging, leading to potentially confounding results.

Given these limitations, we recommend primarily utilizing the HI for simple uni-directional clockwise or counter-clockwise hysteresis patterns in attribution analysis. This focused approach is anticipated to produce more reliable results. With the escalating impact of climate change and increasing human activities, the prevalence of figure-eight and complex hysteresis patterns is on the rise. These patterns often contribute significantly to both runoff volume and sediment transport, necessitating further exploration of their influencing factors. Hence, future research should strive to propose an optimized HI to achieve two goals: (a) accurately calculating HI with minimal observed data and straightforward methods; (b) effectively characterizing the dynamics of figure-eight and complex hysteresis patterns, thereby enhancing their applicability in attribution analysis.

## 5.2. Spatial Distribution and Trends Prediction of Hysteresis Patterns

Current research on hysteresis patterns in hydrological events is largely based on case studies that focus on specific watersheds or regions. These studies are valuable for understanding the localized impacts of climatic and geomorphic factors on sediment transport, but they offer limited insights into the broader spatial distribution of hysteresis patterns. The primary focus has been on regions such as arid and semi-arid zones, with limited attention to other climatic zones like alpine and tropical regions, where different environmental processes may influence hysteresis patterns. As climate change intensifies, more research is beginning to focus on diverse climatic regions, including cold alpine areas and tropical zones, where the mechanisms influencing hydrological events and hysteresis can differ significantly.

However, despite the growing interest in these varied climatic zones, hydrological models have yet to incorporate hysteresis phenomena into hydrological event simulations and sediment transport predictions. Most current models fail to account for the dynamic interactions between discharge ( $Q$ ) and suspended sediment concentration (SSC), particularly the non-linear and time-lag effects that hysteresis patterns reveal. This omission limits the predictive capabilities of these models, especially under the increasingly extreme weather conditions driven by climate change.



The lack of region-specific models that integrate hysteresis dynamics is a critical gap. Given the distinct environmental processes in different climatic and geomorphic regions, there is a clear need to develop regional predictive models tailored to these areas. Such models should incorporate hysteresis factors into their simulations to more accurately predict the behavior of future hydrological events and sediment transport in regions with diverse environmental conditions. For example, the factors driving hysteresis in semi-arid zones, where rainfall intensity and sparse vegetation play key roles, differ significantly from those in alpine regions, where snowmelt and glacial runoff dominate the hydrological response. Similarly, tropical regions, with their distinct precipitation patterns and land-use dynamics, require models that reflect their unique hydrological and sediment transport processes.

In addition to developing regional models, there is also a pressing need to explore the global distribution of hysteresis patterns, much like existing global-scale hydrological studies. While significant progress has been made in understanding local hysteresis patterns, little research has been conducted on how these patterns vary globally. Understanding the global distribution of hysteresis patterns would provide valuable insights into how climate zones, geomorphic settings, and land-use practices interact to influence sediment transport during hydrological events. This type of research would enhance our ability to predict future trends in hydrological events and sediment dynamics on a global scale, contributing to more informed river watershed management and flood mitigation strategies worldwide.

## 6. Conclusions

Hysteresis analysis is widely adopted to elucidate the scattered SSC-Q relationships during hydrological events. This analytical approach aids in the disclosure of sediment sources and transport mechanisms associated with distinct flood types. By consolidating research conducted through hysteresis analysis in diverse river watersheds globally, our review systematically scrutinizes the literature on the principles and applications of this method. The review offers methodological guidance for future analysis of suspended sediment dynamics in hydrological events. The key findings are as follows:

1. Hysteresis patterns play a pivotal role in characterizing the sediment transport process during hydrological events, typically categorized into four main types: clockwise, counter-clockwise, figure-eight, and complex. These diverse hysteresis patterns serve as indicators of distinct sediment source distributions and delivery paths. Specifically, clockwise hysteresis often signifies proximal sediment sources, whereas counter-clockwise hysteresis is commonly associated with upstream or tributary sources. The more intricate sources contribute to the emergence of the figure-eight and complex hysteresis patterns.
2. Quantitative indices of hysteresis index (HI) and flushing index (FI) derived from hysteresis loops serve to characterize the direction, magnitude, and dominance of scouring or deposition within the river channel. This review presents several commonly used hysteresis indices, highlighting their strengths and weaknesses, and assesses their suitability for various hydrological conditions. This comparative analysis offers valuable guidance for researchers in choosing the most appropriate index according to the specific characteristics of both the hydrological event and the watershed.
3. The hysteresis method has been widely applied in hydrological event hydrological studies, facilitating the classification and characterization of hydrological events. It also helps identify key factors influencing these events, such as precipitation intensity, antecedent moisture conditions, and event magnitude, by reflecting sediment sources and transport processes. Additionally, hysteresis analysis is crucial for understanding the main erosion-induced sediment-producing flood types within a watershed, offering valuable insights for guiding watershed management strategies.

This review highlights critical insights into the SSC-Q relationships during hydrological events while acknowledging key challenges that persist. The primary obstacles include the availability of high-resolution data, the development of robust classification methods, and the standardization of quantitative indices for hysteresis analysis. To address these gaps, future research should prioritize the development of regional hydrological models that integrate hysteresis dynamics, enabling more accurate predictions of flood trends and sediment transport. Such advancements are essential for understanding the regional and global distribution of hydrological events, particularly under the influence of climate change. These efforts will provide invaluable guidance for enhancing the effectiveness and sustainability of watershed management practices in the face of evolving environmental conditions.

## Data Availability Statement

This work is a literature review study and does not generate data, models, or code. This review compiles pre-existing information from published works. The publications are available through the DOI links in references.

## Acknowledgments

This work was supported by the National Natural Science Foundation of China (42177335, 41930755, and 42207405).

## References

- Achite, M., & Ouillon, S. (2016). Recent changes in climate, hydrology and sediment load in the Wadi Abd, Algeria (1970–2010). *Hydrology and Earth System Sciences*, 20(4), 1355–1372. <https://doi.org/10.5194/hess-20-1355-2016>
- Aguilera, R., & Melack, J. M. (2018). Concentration-discharge responses to storm events in coastal California watersheds. *Water Resources Research*, 54(1), 407–424. <https://doi.org/10.1002/2017WR021578>
- Ahn, K. H., & Steinschneider, S. (2018). Time-varying suspended sediment-discharge rating curves to estimate climate impacts on fluvial sediment transport. *Hydrological Processes*, 32(1), 102–117. <https://doi.org/10.1002/hyp.11402>
- Aich, V., Zimmermann, A., & Elsenbeer, H. (2014). Quantification and interpretation of suspended-sediment discharge hysteresis patterns: How much data do we need? *Catena*, 122, 120–129. <https://doi.org/10.1016/j.catena.2014.06.020>
- Alavez-Vargas, M., Birkel, C., Corona, A., & Agustin Brena-Naranjo, J. (2021). Land cover change induced sediment transport behaviour in a large tropical Mexican catchment. *Hydrological Sciences Journal*, 66(6), 1069–1082. <https://doi.org/10.1080/02626667.2021.1903472>
- Alexandrov, Y., Laronne, J. B., & Reid, I. (2007). Intra-event and inter-seasonal behaviour of suspended sediment in flash floods of the semi-arid northern Negev, Israel. *Geomorphology*, 85(1–2), 85–97. <https://doi.org/10.1016/j.geomorph.2006.03.013>
- Al Sawaf, F., Al Ghandour, F., Masoud, O., & Al Kayed, A. (2024). Examining the relationship between rainfall, runoff, and turbidity during the rainy season in coastal zones of Oman. *GeoHazards*, 7(1), 112–126. <https://doi.org/10.3390/geoHazards7010008>
- Ares, M. G., Varni, M., & Chagas, C. (2016). Suspended sediment concentration controlling factors: An analysis for the Argentine pampas region. *Hydrological Sciences Journal*, 61(12), 2237–2248. <https://doi.org/10.1080/02626667.2015.1099793>
- Asselman, N. E. M. (1999). Suspended sediment dynamics in a large drainage basin: The River Rhine. *Hydrological Processes*, 13(10), 1437–1450. [https://doi.org/10.1002/\(SICI\)1099-1085\(199907\)13:10<1437::AID-HYP821>3.0.CO;2-J](https://doi.org/10.1002/(SICI)1099-1085(199907)13:10<1437::AID-HYP821>3.0.CO;2-J)
- Baca, P. (2008). Hysteresis effect in suspended sediment concentration in the Rybarik basin, Slovakia. *Hydrological Sciences Journal*, 53(1), 224–235. <https://doi.org/10.1623/hysj.53.1.224>
- Baker, E. B., & Showers, W. J. (2019). Hysteresis analysis of nitrate dynamics in the Neuse River, NC. *Science of the Total Environment*, 652, 889–899. <https://doi.org/10.1016/j.scitotenv.2018.10.254>
- Baloul, D., Ghenim, A. N., & Megnounif, A. (2024). Q-SSC behavior during floods in the Isser watershed, north-west of Algeria. *Polish Journal of Environmental Studies*, 33(5), 5567–5576. <https://doi.org/10.15244/pjoes/185705>
- Banasik, K., & Hejduk, A. (2015). Ratio of basin lag times for runoff and sediment yield processes recorded in various environments. *Proceedings of the IAHS*, 367, 163–169. <https://doi.org/10.5194/piahs-367-163-2015>
- Banasik, K., Madeyski, M., Mitchell, J. K., & Mori, K. (2005). An investigation of lag times for rainfall–runoff–sediment yield events in small river basins. *Hydrological Sciences Journal*, 50(5), 866. <https://doi.org/10.1623/hysj.2005.50.5.857>
- Banasik, K., & Walling, D. E. (1996). Predicting sediment graphs for a small agricultural catchment. *Hydrology Research*, 27(4), 275–294. <https://doi.org/10.2166/nh.1996.0010>
- Baniya, S., Maharjan, A., Dahal, K. R., & Shrestha, S. (2024). Effects of rainfall on fluvial discharge and suspended sediment transport in the Central Himalayan region. *Theoretical and Applied Climatology*, 150(1), 22–35. <https://doi.org/10.1007/s00704-023-04680-5>
- Bender, M. A., dos Santos, D. R., Tiecher, T., Gomes Minella, J. P., Peixoto de Barros, C. A., & Ramon, R. (2018). Phosphorus dynamics during storm events in a subtropical rural catchment in southern Brazil. *Agriculture, Ecosystems & Environment*, 261, 93–102. <https://doi.org/10.1016/j.agee.2018.04.004>
- Bettel, L., Fox, J., Husic, A., Zhu, J. F., Aamery, N. A., Mahoney, T., & Gold-McCoy, A. (2022). Sediment transport investigation in a karst aquifer hypothesizes controls on internal versus external sediment origin and saturation impact on hysteresis. *Journal of Hydrology*, 613, 128391. <https://doi.org/10.1016/j.jhydrol.2022.128391>
- Bieroza, M. Z., & Heathwaite, A. L. (2015). Seasonal variation in phosphorus concentration-discharge hysteresis inferred from high-frequency in situ monitoring. *Journal of Hydrology*, 524, 333–347. <https://doi.org/10.1016/j.jhydrol.2015.02.036>
- Blothe, J. H., & Hoffmann, T. (2022). Spatio-temporal differences dominate suspended sediment dynamics in medium-sized catchments in central Germany. *Geomorphology*, 418, 108462. <https://doi.org/10.1016/j.geomorph.2022.108462>
- Bolade, O., & Hansen, A. T. (2023). Inferring drivers of nitrate and sediment event dynamics from hysteresis metrics for two large agricultural watersheds. *Hydrological Processes*, 37(9), e14969. <https://doi.org/10.1002/hyp.14969>
- Bowes, M. J., House, W. A., Hodgkinson, R. A., & Leach, D. V. (2005). Phosphorus-discharge hysteresis during storm events along a river catchment: The river Swale, UK. *Water Research*, 39(5), 751–762. <https://doi.org/10.1016/j.watres.2004.11.027>
- Buendia, C., Vericat, D., Batalla, R. J., & Gibbins, C. N. (2016). Temporal dynamics of sediment transport and transient in-channel storage in a highly erodible catchment. *Land Degradation & Development*, 27(4), 1045–1063. <https://doi.org/10.1002/ldr.2348>
- Burt, T. P., Donohoe, M. A., & Vann, A. R. (1983). The effect of forestry drainage operations on upland sediment yields: The results of a storm-based study. *Earth Surface Processes and Landforms*, 8(4), 339–346. <https://doi.org/10.1002/esp.3290080406>
- Burt, T. P., Worrall, F., Howden, N. J. K., & Anderson, M. G. (2015). Shifts in discharge-concentration relationships as a small catchment recovers from severe drought. *Hydrological Processes*, 29(4), 498–507. <https://doi.org/10.1002/hyp.10169>
- Cao, L., Liu, S., Wang, S., Cheng, Q., Fryar, A. E., Zhang, L., et al. (2021). Factors controlling discharge-suspended sediment hysteresis in karst basins, southwest China: Implications for sediment management. *Journal of Hydrology*, 594, 125792. <https://doi.org/10.1016/j.jhydrol.2020.125792>
- Carrillo, R., & Mao, L. (2020). Coupling sediment transport dynamics with sediment and discharge sources in a glacial Andean basin. *Water*, 12(12), 3452. <https://doi.org/10.3390/w12123452>
- Chen, J., & Chang, H. (2019). Dynamics of wet-season turbidity in relation to precipitation, discharge, and land cover in three urbanizing watersheds, Oregon. *River Research and Applications*, 35(7), 892–904. <https://doi.org/10.1002/rra.3487>
- Cheraghi, M., Jomaa, S., Sander, G. C., & Barry, D. A. (2016). Hysteretic sediment fluxes in rainfall-driven soil erosion: Particle size effects. *Water Resources Research*, 52(11), 8613–8629. <https://doi.org/10.1002/2016WR019314>
- Coch, C., Lamoureux, S. F., Knoblauch, C., Eischeid, I., Fritz, M., Obu, J., & Lantuit, H. (2018). Summer rainfall dissolved organic carbon, solute, and sediment fluxes in a small Arctic coastal catchment on Herschel Island (Yukon Territory, Canada). *Arctic Science*, 4(4), 750–780. <https://doi.org/10.1139/as-2018-0010>

- Collins, A. L., & Walling, D. E. (2004). Documenting catchment suspended sediment sources: Problems, approaches and prospects. *Progress in Physical Geography: Earth and Environment*, 28(2), 159–196. <https://doi.org/10.1191/0309133304pp409ra>
- Collins, M. B. (1981). Sediment yield studies of headwater catchments in Sussex, S.E. England. *Earth Surface Processes and Landforms*, 6, 517–539. <https://doi.org/10.1002/esp.3290060603>
- De Girolamo, A. M., Pappagallo, G., & Lo Porto, A. (2015). Temporal variability of suspended sediment transport and rating curves in a Mediterranean river basin: The Celone (SE Italy). *Catena*, 128, 135–143. <https://doi.org/10.1016/j.catena.2014.09.020>
- de Menezes, D., Minella, J. P. G., & Tassi, R. (2020). Monitoring sediment yield for soil and water conservation planning in rural catchments. *Environmental Monitoring and Assessment*, 192(11), 736. <https://doi.org/10.1007/s10661-020-08670-y>
- Diaf, M., Hazzab, A., Yahiaoui, A., & Belkendil, A. (2020). Characterization and frequency analysis of flooding solid flow in semi-arid zone: Case of Mekerra catchment in the north-west of Algeria. *Applied Water Science*, 10(2), 59. <https://doi.org/10.1007/s13201-019-1132-4>
- di Cenzo, P. D., & Luk, S. (1997). Gully erosion and sediment transport in a small subtropical catchment, South China. *Catena*, 29(2), 161–176. [https://doi.org/10.1016/S0341-8162\(96\)00053-7](https://doi.org/10.1016/S0341-8162(96)00053-7)
- Di Pillo, R., De Girolamo, A. M., Lo Porto, A., & Todisco, M. T. (2023). Detecting the drivers of suspended sediment transport in an intermittent river: An event-based analysis. *Catena*, 222, 106881. <https://doi.org/10.1016/j.catena.2022.106881>
- Domingo, J. P. T., Attal, M., Mudd, S. M., Ngwenya, B. T., & David, C. P. C. (2021). Seasonal fluxes and sediment routing in tropical catchments affected by nickel mining. *Earth Surface Processes and Landforms*, 46(13), 2632–2655. <https://doi.org/10.1002/esp.5198>
- Dominic, J. A., Aris, A. Z., & Sulaiman, W. N. A. (2015). Factors controlling the suspended sediment yield during rainfall events of dry and wet weather conditions in A tropical urban catchment. *Water Resources Management*, 29(12), 4519–4538. <https://doi.org/10.1007/s11269-015-1073-0>
- Doomen, A. M. C., Wijma, E., Zwolsman, J. J. G., & Middelkoop, H. (2008). Predicting suspended sediment concentrations in the Meuse River using a supply-based rating curve. *Hydrological Processes*, 22(12), 1846–1856. <https://doi.org/10.1002/hyp.6767>
- Dumitriu, D. (2020). Sediment flux during flood events along the Trotuş river channel: Hydrogeomorphological approach. *Journal of Soils and Sediments*, 20(11), 4083–4102. <https://doi.org/10.1007/s11368-020-02688-4>
- Dupas, R., Gascuel-Oudou, C., Gilliet, N., Grimaldi, C., & Gruau, G. (2015). Distinct export dynamics for dissolved and particulate phosphorus reveal independent transport mechanisms in an arable headwater catchment. *Hydrological Processes*, 29(14), 3162–3178. <https://doi.org/10.1002/hyp.10432>
- Duvert, C., Gratiot, N., Evrard, O., Navratil, O., Nemery, J., Prat, C., & Esteves, M. (2010). Drivers of erosion and suspended sediment transport in three headwater catchments of the Mexican Central Highlands. *Geomorphology*, 123(3–4), 243–256. <https://doi.org/10.1016/j.geomorph.2010.07.016>
- El Azzzi, D., Probst, J. L., Teisserenc, R., Merlina, G., Baqué, D., Julien, F., et al. (2016). Trace element and pesticide dynamics during a flood event in the Save agricultural watershed: Soil–river transfer pathways and controlling factors. *Water, Air, & Soil Pollution*, 227(442), 442. <https://doi.org/10.1007/s11270-016-3111-0>
- Engel, M., Coviello, V., Savi, S., Buter, A., Andreoli, A., Miyata, S., et al. (2024). Meltwater-driven sediment transport dynamics in two contrasting alpine proglacial streams. *Journal of Hydrology*, 635, 131171. <https://doi.org/10.1016/j.jhydrol.2024.131171>
- Esteves, M., Legout, C., Navratil, O., & Evrard, O. (2019). Medium term high frequency observation of discharges and suspended sediment in a Mediterranean mountainous catchment. *Journal of Hydrology*, 568, 562–574. <https://doi.org/10.1016/j.jhydrol.2018.10.066>
- Fan, X., Shi, C., Shao, W., & Zhou, Y. (2013). The suspended sediment dynamics in the Inner-Mongolia reaches of the upper Yellow River. *Catena*, 109, 72–82. <https://doi.org/10.1016/j.catena.2013.05.010>
- Fang, H. (2019). Temporal changes in suspended sediment transport during the past five decades in a mountainous catchment, eastern China. *Journal of Soils and Sediments*, 19(12), 4073–4085. <https://doi.org/10.1007/s11368-019-02363-x>
- Fang, H. Y., Cai, Q. G., Chen, H., & Li, Q. Y. (2008). Temporal changes in suspended sediment transport in a gullied loess basin: The lower Chabagou Creek on the loess plateau in China. *Earth Surface Processes and Landforms*, 33(13), 1977–1992. <https://doi.org/10.1002/esp.1649>
- Fang, N. F., Shi, Z. H., Chen, F. X., Zhang, H. Y., & Wang, Y. X. (2015). Discharge and suspended sediment patterns in a small mountainous watershed with widely distributed rock fragments. *Journal of Hydrology*, 528, 238–248. <https://doi.org/10.1016/j.jhydrol.2015.06.046>
- Fang, N. F., Shi, Z. H., Li, L., & Jiang, C. (2011). Rainfall, runoff, and suspended sediment delivery relationships in a small agricultural watershed of the Three Gorges area, China. *Geomorphology*, 135(1–2), 158–166. <https://doi.org/10.1016/j.geomorph.2011.08.013>
- Favaro, E. A., & Lamoureux, S. F. (2015). Downstream patterns of suspended sediment transport in a High Arctic river influenced by permafrost disturbance and recent climate change. *Geomorphology*, 246, 359–369. <https://doi.org/10.1016/j.geomorph.2015.06.038>
- Fortesa, J., Latron, J., Garcia-Comendador, J., Company, J., & Estrany, J. (2020). Runoff and soil moisture as driving factors in suspended sediment transport of a small mid-mountain Mediterranean catchment. *Geomorphology*, 368, 107349. <https://doi.org/10.1016/j.geomorph.2020.107349>
- Fortesa, J., Ricci, G. F., Garcia-Comendador, J., Gentile, F., Estrany, J., Sauquet, E., et al. (2021). Analysing hydrological and sediment transport regime in two Mediterranean intermittent rivers. *Catena*, 196, 104865. <https://doi.org/10.1016/j.catena.2020.104865>
- Gao, G., Fu, B., Zhang, J., Ma, Y., & Sivapalan, M. (2018). Multiscale temporal variability of flow–sediment relationships during the 1950s–2014 in the Loess Plateau, China. *Journal of Hydrology*, 563, 609–619. <https://doi.org/10.1016/j.jhydrol.2018.06.044>
- Gao, P., & Josefson, M. (2012). Event-based suspended sediment dynamics in a central New York watershed. *Geomorphology*, 139, 425–437. <https://doi.org/10.1016/j.geomorph.2011.11.007>
- Gao, P., Nearing, M. A., & Commons, M. (2013). Suspended sediment transport at the instantaneous and event time scales in semiarid watersheds of southeastern Arizona, USA. *Water Resources Research*, 49(10), 6857–6870. <https://doi.org/10.1002/wrcr.20549>
- Garcia-Comendador, J., Martinez-Carreras, N., Fortesa, J., Company, J., Borrás, A., & Estrany, J. (2021). Combining sediment fingerprinting and hydro-sedimentary monitoring to assess suspended sediment provenance in a mid-mountainous Mediterranean catchment. *Journal of Environmental Management*, 299, 113593. <https://doi.org/10.1016/j.jenvman.2021.113593>
- Garcia-Rama, A., Pagano, S. G., Gentile, F., & Lenzi, M. A. (2016). Suspended sediment transport analysis in two Italian instrumented catchments. *Journal of Mountain Science*, 13(6), 957–970. <https://doi.org/10.1007/s11629-016-3858-x>
- Geeraert, N., Omengo, F. O., Tamooh, F., Paron, P., Bouillon, S., & Govers, G. (2015). Sediment yield of the lower Tana river, Kenya, is insensitive to dam construction: Sediment mobilization processes in a semi-arid tropical river system. *Earth Surface Processes and Landforms*, 40(13), 1827–1838. <https://doi.org/10.1002/esp.3763>
- Gellis, A. C. (2013). Factors influencing storm-generated suspended-sediment concentrations and loads in four basins of contrasting land use, humid-tropical Puerto Rico. *Catena*, 104, 39–57. <https://doi.org/10.1016/j.catena.2012.10.018>
- Ghimire, S., Singh, U., Panthi, K. K., & Bhattarai, P. K. (2024). Suspended sediment source and transport mechanisms in a Himalayan river. *Water*, 16(7), 1063. <https://doi.org/10.3390/w16071063>

- Ghosh, K., & Munoz-Arriola, F. (2023). Hysteresis and streamflow-sediment relations across the pre-to-post dam construction continuum in a highly regulated transboundary Himalayan River basin. *Journal of Hydrology*, 624, 129885. <https://doi.org/10.1016/j.jhydrol.2023.129885>
- Gimenez, R., Casali, J., Grande, I., Diez, J., Campo, M. A., Alvarez-Mozos, J., & Goni, M. (2012). Factors controlling sediment export in a small agricultural watershed in Navarre (Spain). *Agricultural Water Management*, 110, 1–8. <https://doi.org/10.1016/j.agwat.2012.03.007>
- Goodwin, T. H., Young, A. R., Holmes, M. G. R., Old, G. H., Hewitt, N., Leeks, G. J. L., et al. (2003). The temporal and spatial variability of sediment transport and yields within the Bradford Beck catchment, West Yorkshire. *The Science of the Total Environment*, 314–316, 475–494. [https://doi.org/10.1016/S0048-9697\(03\)00069-X](https://doi.org/10.1016/S0048-9697(03)00069-X)
- Gray, A. B., Warrick, J. A., Pasternack, G. B., Watson, E. B., & Gofii, M. A. (2014). Suspended sediment behaviour in a coastal dry-summer subtropical catchment: Effects of hydrologic preconditions. *Geomorphology*, 214, 485–501. <https://doi.org/10.1016/j.geomorph.2014.03.009>
- Grimshaw, D. L., & Lewin, J. (1980). Source identification for suspended sediments. *Journal of Hydrology*, 47(1), 151–162. [https://doi.org/10.1016/0022-1694\(80\)90053-0](https://doi.org/10.1016/0022-1694(80)90053-0)
- Haddadchi, A., & Hicks, M. (2021). Interpreting event-based suspended sediment concentration and flow hysteresis patterns. *Journal of Soils and Sediments*, 21(1), 592–612. <https://doi.org/10.1007/s11368-020-02777-y>
- Hamshaw, S. D., Dewoolkar, M. M., Schroth, A. W., Wemple, B. C., & Rizzo, D. M. (2018). A new machine-learning approach for classifying hysteresis in suspended-sediment discharge relationships using high-frequency monitoring data. *Water Resources Research*, 54(6), 4040–4058. <https://doi.org/10.1029/2017WR022238>
- Hapsari, D., Onishi, T., Imaizumi, F., Noda, K., & Senge, M. (2019). The use of sediment rating curve under its limitations to estimate the suspended load. *Reviews in Agricultural Science*, 7(0), 88–101. [https://doi.org/10.7831/ras.7.0\\_88](https://doi.org/10.7831/ras.7.0_88)
- Heathwaite, A. L., & Bierzo, M. (2021). Fingerprinting hydrological and biogeochemical drivers of freshwater quality. *Hydrological Processes*, 35(1). <https://doi.org/10.1002/hyp.13973>
- Heidel, S. G. (1956). The progressive lag of sediment concentration with flood waves. *Transactions - American Geophysical Union*, 37(1), 56. <https://doi.org/10.1029/TR037i001p00056>
- Herrero, A., Vila, J., Eljarrat, E., Ginebreda, A., Sabater, S., Batalla, R. J., & Barcelo, D. (2018). Transport of sediment borne contaminants in a Mediterranean river during a high flow event. *Science of the Total Environment*, 633, 1392–1402. <https://doi.org/10.1016/j.scitotenv.2018.03.205>
- Horowitz, A. J., Clarke, R. T., & Merten, G. H. (2015). The effects of sample scheduling and sample numbers on estimates of the annual fluxes of suspended sediment in fluvial systems. *Hydrological Processes*, 29(4), 531–543. <https://doi.org/10.1002/hyp.10172>
- Hu, J., Gao, P., Mu, X., Zhao, G., Sun, W., Li, P., & Zhang, L. (2019). Runoff-sediment dynamics under different flood patterns in a Loess Plateau catchment, China. *Catena*, 173, 234–245. <https://doi.org/10.1016/j.catena.2018.10.023>
- Huang, X., Fang, N. F., Zhu, T. X., Wang, L., Shi, Z. H., & Hua, L. (2018). Hydrological response of a large-scale mountainous watershed to rainstorm spatial patterns and reforestation in subtropical China. *Science of the Total Environment*, 645, 1083–1093. <https://doi.org/10.1016/j.scitotenv.2018.07.248>
- Hudson, P. F. (2003). Event sequence and sediment exhaustion in the lower Panuco Basin, Mexico. *Catena*, 52(1), 57–76. [https://doi.org/10.1016/S0341-8162\(02\)00145-5](https://doi.org/10.1016/S0341-8162(02)00145-5)
- Hughes, A. O., Quinn, J. M., & McKergow, L. A. (2012). Land use influences on suspended sediment yields and event sediment dynamics within two headwater catchments, Waikato, New Zealand. *New Zealand Journal of Marine & Freshwater Research*, 46(3), 315–333. <https://doi.org/10.1080/00288330.2012.661745>
- Irvine, K. N., & Drake, J. J. (1987). Process-oriented estimation of suspended sediment concentration. *Journal of the American Water Resources Association*, 23(6), 1017–1025. <https://doi.org/10.1111/j.1752-1688.1987.tb00851.x>
- Jansson, M. B. (1996). Estimating a sediment rating curve of the Reventazón river at Palomo using logged mean loads within discharge classes. *Journal of Hydrology*, 183(3–4), 227–241. [https://doi.org/10.1016/0022-1694\(95\)02988-5](https://doi.org/10.1016/0022-1694(95)02988-5)
- Jansson, M. B. (2002). Determining sediment source areas in a tropical river basin, Costa Rica. *Catena*, 47(1), 63–84. [https://doi.org/10.1016/S0341-8162\(01\)00173-4](https://doi.org/10.1016/S0341-8162(01)00173-4)
- Javed, A., Hamshaw, S. D., Lee, B. S., & Rizzo, D. M. (2021). Multivariate event time series analysis using hydrological and suspended sediment data. *Journal of Hydrology*, 593, 125802. <https://doi.org/10.1016/j.jhydrol.2020.125802>
- Jeje, L. K., Ogunkoya, O. O., & Oluwatimilehin, J. M. (1991). Variation in suspended sediment concentration during storm discharges in three small streams in upper osun basin, Central Western Nigeria. *Hydrological Processes*, 5(4), 361–369. <https://doi.org/10.1002/hyp.3360050404>
- Juez, C., Hassan, M. A., & Franca, M. J. (2018). The origin of fine sediment determines the observations of suspended sediment fluxes under unsteady flow conditions. *Water Resources Research*, 54(8), 5654–5669. <https://doi.org/10.1029/2018WR022982>
- Katebikord, A., Sadeghi, S. H., & Singh, V. P. (2024). A new approach to simulate watershed sediment graphs. *International Journal of Sediment Research*, 39(1), 153–164. <https://doi.org/10.1016/j.ijsrc.2023.11.002>
- Keesstra, S. D., Davis, J., Masselink, R. H., Casali, J., Peeters, E. T. H. M., & Dijkma, R. (2019). Coupling hysteresis analysis with sediment and hydrological connectivity in three agricultural catchments in Navarre, Spain. *Journal of Soils and Sediments*, 19(3), 1598–1612. <https://doi.org/10.1007/s11368-018-02223-0>
- Kelly, L. A. (1992). Estimating sediment yield variation in a small forested upland catchment. *Hydrobiologia*, 235(1), 199–203. <https://doi.org/10.1007/BF00026212>
- Klein, M. (1984). Anti clockwise hysteresis in suspended sediment concentration during individual storms: Holbeck catchment; Yorkshire, England. *Catena*, 11(2–3), 251–257. [https://doi.org/10.1016/0341-8162\(84\)90014-6](https://doi.org/10.1016/0341-8162(84)90014-6)
- Krajewski, A., Gładcki, J., & Banasik, K. (2018). Transport of suspended sediment during flood events in a small urban catchment. *Acta Scientiarum Polonorum Formatio Circumiectionis*, 17(3), 119–127. <https://doi.org/10.15576/ASP.FC/2018.17.3.119>
- Landers, M. N., & Sturm, T. W. (2013). Hysteresis in suspended sediment to turbidity relations due to changing particle size distributions. *Water Resources Research*, 49(9), 5487–5500. <https://doi.org/10.1002/wrcr.20394>
- Langlois, J. L., Johnson, D. W., & Mehuys, G. R. (2005). Suspended sediment dynamics associated with snowmelt runoff in a small mountain stream of Lake Tahoe (Nevada). *Hydrological Processes*, 19(18), 3569–3580. <https://doi.org/10.1002/hyp.5844>
- Lannergard, E. E., Folster, J., & Futter, M. N. (2021). Turbidity-discharge hysteresis in a meso-scale catchment: The importance of intermediate scale events. *Hydrological Processes*, 35(12). <https://doi.org/10.1002/hyp.14435>
- Lawler, D. M., Petts, G. E., Foster, I. D. L., & Harper, S. (2006). Turbidity dynamics during spring storm events in an urban headwater river system: The Upper Tame, West Midlands, UK. *Science of the Total Environment*, 360(1–3), 109–126. <https://doi.org/10.1016/j.scitotenv.2005.08.032>
- Lefrancois, J., Grimaldi, C., Gascuel-Oudoux, C., & Gilliet, N. (2007). Suspended sediment and discharge relationships to identify bank degradation as a main sediment source on small agricultural catchments. *Hydrological Processes*, 21(21), 2923–2933. <https://doi.org/10.1002/hyp.6509>

- Lenzi, M. A., & Marchi, L. (2000). Suspended sediment load during floods in a small stream of the Dolomites (northeastern Italy). *Catena*, 39(4), 267–282. [https://doi.org/10.1016/S0341-8162\(00\)00079-5](https://doi.org/10.1016/S0341-8162(00)00079-5)
- Li, D., Lu, X., Overeem, I., Walling, D. E., Syvitski, J., Kettner, A. J., et al. (2021). Exceptional increases in fluvial sediment fluxes in a warmer and wetter high Mountain Asia. *Science*, 374(6567), 599–603. <https://doi.org/10.1126/science.abi9649>
- Li, X., Ren, J., Xue, J., Xu, Q., Yuan, J., & Zhang, W. (2024). Interpretation of delayed suspended sediment transport during flood events from the perspective of movement characteristics. *Journal of Hydrology*, 644, 132127. <https://doi.org/10.1016/j.jhydrol.2024.132127>
- Li, Z., Xu, X., Zhu, J., Xu, C., & Wang, K. (2019). Effects of lithology and geomorphology on sediment yield in karst mountainous catchments. *Geomorphology*, 343, 119–128. <https://doi.org/10.1016/j.geomorph.2019.07.001>
- Liu, F., Hu, S., Guo, X. J., Luo, X. X., Cai, H. Y., & Yang, Q. S. (2017). Recent changes in the sediment regime of the pearl river (south China): Causes and implications for the pearl river delta. *Hydrological Processes*, 32(12), 1771–1785. <https://doi.org/10.1002/hyp.11513>
- Liu, W., Birgand, F., Tian, S., & Chen, C. (2021). Event-scale hysteresis metrics to reveal processes and mechanisms controlling constituent export from watersheds: A review. *Water Research*, 200, 117254. <https://doi.org/10.1016/j.watres.2021.117254>
- Lloyd, C. E. M., Freer, J. E., Johns, P. J., & Collins, A. L. (2016a). Technical note: Testing an improved index for analysing storm discharge-concentration hysteresis. *Hydrology and Earth System Sciences*, 20(2), 625–632. <https://doi.org/10.5194/hess-20-625-2016>
- Lloyd, C. E. M., Freer, J. E., Johns, P. J., & Collins, A. L. (2016b). Using hysteresis analysis of high-resolution water quality monitoring data, including uncertainty, to infer controls on nutrient and sediment transfer in catchments. *Science of the Total Environment*, 543, 388–404. <https://doi.org/10.1016/j.scitotenv.2015.11.028>
- Londero, A. L., Minella, J. P. G., Deuschle, D., Schneider, F. J. A., Boeni, M., & Merten, G. H. (2018). Impact of broad-based terraces on water and sediment losses in no-till (paired zero-order) catchments in southern Brazil. *Journal of Soils and Sediments*, 18(3), 1159–1175. <https://doi.org/10.1007/s11368-017-1886-8>
- Long, D., Pan, M., Dong, S., & Wu, Z. (2024). Suspended sediment-discharge hysteresis characteristics and controlling factors in a small watershed, Southeastern China. *Catena*, 227, 107114. <https://doi.org/10.1016/j.catena.2023.107114>
- Lopez-Tarazon, J. A., Batalla, R. J., Vericat, D., & Francke, T. (2009). Suspended sediment transport in a highly erodible catchment: The River Isabena (Southern Pyrenees). *Geomorphology*, 109(3–4), 210–221. <https://doi.org/10.1016/j.geomorph.2009.03.003>
- Lopez-Tarazon, J. A., & Estrany, J. (2017). Exploring suspended sediment delivery dynamics of two Mediterranean nested catchments. *Hydrological Processes*, 31(3), 698–715. <https://doi.org/10.1002/hyp.11069>
- Lyu, Y., Fagherazzi, S., Zheng, S., Tan, G., & Shu, C. (2020). Enhanced hysteresis of suspended sediment transport in response to upstream damming: An example of the middle Yangtze River downstream of the Three Gorges Dam. *Earth Surface Processes and Landforms*, 45(8), 1846–1859. <https://doi.org/10.1002/esp.4850>
- Malutta, S., Kobiyama, M., Chaffé, P. L. B., & Bonuma, N. B. (2020). Hysteresis analysis to quantify and qualify the sediment dynamics: State of the art. *Water Science and Technology*, 81(12), 2471–2487. <https://doi.org/10.2166/wst.2020.279>
- Mano, V., Nemery, J., Belleudy, P., & Poirel, A. (2009). Assessment of suspended sediment transport in four alpine watersheds (France): Influence of the climatic regime. *Hydrological Processes*, 23(5), 777–792. <https://doi.org/10.1002/hyp.7178>
- Manseau, F., Bhiry, N., Molson, J., & Cloutier, D. (2022). Factors affecting river turbidity in a degrading permafrost environment: The Tasiapik River, Umiujaq (Nunavik). *Arctic Science*, 8(4), 1202–1216. <https://doi.org/10.1139/as-2021-0036>
- Marin-Ramirez, A., Mahoney, D. T., Riddle, B., Bettel, L., & Fox, J. F. (2024). Response time of fast flowing hydrologic pathways controls sediment hysteresis in a low-gradient watershed, as evidenced from tracer results and machine learning models. *Journal of Hydrology*, 645, 132207. <https://doi.org/10.1016/j.jhydrol.2024.132207>
- Martin, S. E., Conklin, M. H., & Bales, R. C. (2014). Seasonal accumulation and depletion of local sediment stores of four headwater catchments. *Water*, 6(7), 2144–2163. <https://doi.org/10.3390/w6072144>
- Megnounif, A., Terfous, A., & Ouillon, S. (2013). A graphical method to study suspended sediment dynamics during flood events in the Wadi Seboudou, NW Algeria (1973–2004). *Journal of Hydrology*, 497, 24–36. <https://doi.org/10.1016/j.jhydrol.2013.05.029>
- Mihiranga, H. K. M., Jiang, Y., Li, X., Wang, W., De Silva, K., Kumwimba, M. N., et al. (2021). Nitrogen/phosphorus behaviour traits and implications during storm events in a semi-arid mountainous watershed. *Science of the Total Environment*, 791, 148382. <https://doi.org/10.1016/j.scitotenv.2021.148382>
- Millares, A., & Monino, A. (2020). Hydro-meteorological drivers influencing suspended sediment transport and yield in a semi-arid mountainous basin. *Earth Surface Processes and Landforms*, 45(15), 3791–3807. <https://doi.org/10.1080/02626667.2020.1724294>
- Misset, C., Recking, A., Legout, C., Poirel, A., Cazilhac, M., Esteves, M., & Bertrand, M. (2019). An attempt to link suspended load hysteresis patterns and sediment sources configuration in alpine catchments. *Journal of Hydrology*, 576, 72–84. <https://doi.org/10.1016/j.jhydrol.2019.06.039>
- Nadal-Romero, E., Reguees, D., & Latron, J. (2008). Relationships among rainfall, runoff, and suspended sediment in a small catchment with badlands. *Catena*, 74(2), 127–136. <https://doi.org/10.1016/j.catena.2008.03.014>
- Ourng, C., Sauvage, S., Coynel, A., Maneux, E., Etcheber, H., & Sanchez-Perez, J. M. (2011). Fluvial transport of suspended sediment and organic carbon during flood events in a large agricultural catchment in southwest France. *Hydrological Processes*, 25(15), 2365–2378. <https://doi.org/10.1002/hyp.7999>
- Ourng, C., Sauvage, S., & Sanchez-Perez, J. M. (2010). Dynamics of suspended sediment transport and yield in a large agricultural catchment, southwest France. *Earth Surface Processes and Landforms*, 35(11), 1289–1301. <https://doi.org/10.1002/esp.1971>
- Overeem, I., Hudson, B. D., Syvitski, J. P. M., Mikkelsen, A. B., Hasholt, B., van den Broeke, M. R., et al. (2017). Substantial export of suspended sediment to the global oceans from glacial erosion in Greenland. *Nature Geoscience*, 10(11), 859–863. <https://doi.org/10.1038/ngeo3046>
- Pagano, S. G., Rainato, R., Garcia-Rama, A., Gentile, F., & Lenzi, M. A. (2019). Analysis of suspended sediment dynamics at event scale: Comparison between a mediterranean and an alpine basin. *Hydrological Sciences Journal*, 64(8), 948–961. <https://doi.org/10.1080/02626667.2019.1606428>
- Paustian, S. J., & Beschta, R. L. (1979). The suspended sediment regime of an Oregon coast range stream. *JAWRA Journal of the American Water Resources Association*, 15(1), 144–154. <https://doi.org/10.1111/j.1752-1688.1979.tb00295.x>
- Pellegrini, G., Mao, L., Rainato, R., & Picco, L. (2023). Surprising suspended sediment dynamics of an alpine basin affected by a large infrequent disturbance. *Journal of Hydrology*, 617, 128933. <https://doi.org/10.1016/j.jhydrol.2022.128933>
- Perks, M. T., Owen, G. J., Benskin, C. M. H., Jonczyk, J., Deasy, C., Burke, S., et al. (2015). Dominant mechanisms for the delivery of fine sediment and phosphorus to fluvial networks draining grassland dominated headwater catchments. *Science of the Total Environment*, 523, 178–190. <https://doi.org/10.1016/j.scitotenv.2015.03.008>
- Pickering, C., & Ford, W. I. (2021). Effect of watershed disturbance and river-tributary confluences on watershed sedimentation dynamics in the Western Allegheny Plateau. *Journal of Hydrology*, 602, 126784. <https://doi.org/10.1016/j.jhydrol.2021.126784>

- Pietron, J., Jarsjo, J., Romanchenko, A. O., & Chalov, S. R. (2015). Model analyses of the contribution of in-channel processes to sediment concentration hysteresis loops. *Journal of Hydrology*, 527, 576–589. <https://doi.org/10.1016/j.jhydrol.2015.05.009>
- Pulley, S., Goubet, A., Moser, I., Browning, S., & Collins, A. L. (2019). The sources and dynamics of fine-grained sediment degrading the Freshwater Pearl Mussel (*Margaritifera margaritifera*) beds of the River Torridge, Devon, UK. *Science of the Total Environment*, 657, 420–434. <https://doi.org/10.1016/j.scitotenv.2018.11.401>
- Ram, A. R., & Terry, J. P. (2016). Stream turbidity responses to storm events in a pristine rainforest watershed on the Coral Coast of southern Fiji. *International Journal of Sediment Research*, 31(4), 279–290. <https://doi.org/10.1016/j.ijsrc.2016.07.002>
- Ranjan, R., & Roshni, D. (2024). Potential variability of discharge and suspended sediment dynamics in a tropical river basin under changing climate conditions. *Environmental Earth Sciences*, 83(6), 409. <https://doi.org/10.1007/s12665-024-11688-9>
- Ren, J., Zhao, M., Zhang, W., Xu, Q., Yuan, J., & Dong, B. (2020). Impact of the construction of cascade reservoirs on suspended sediment peak transport variation during flood events in the Three Gorges Reservoir. *Catena*, 188, 104409. <https://doi.org/10.1016/j.catena.2019.104409>
- Rendon-Herrero, O. (1974). Estimation of washload produced on certain small watersheds. *Journal of the Hydraulics Division*, 100(7), 835–848. <https://doi.org/10.1061/JYCEAJ.0004005>
- Rendon-Herrero, O. (1978). Unit sediment graph. *Water Resources Research*, 14(5), 889–901. <https://doi.org/10.1029/WR014i005p00889>
- Richards, G., & Moore, R. D. (2003). Suspended sediment dynamics in a steep, glacier-fed mountain stream, Place Creek, Canada. *Hydrological Processes*, 17(9), 1733–1753. <https://doi.org/10.1002/hyp.1208>
- Richards, K. (1984). Some observations on suspended sediment dynamics in Storbregrova, Jotunheimen. *Earth Surface Processes and Landforms*, 9(2), 101–112. <https://doi.org/10.1002/esp.3290090202>
- Riihimäki, C. A., MacGregor, K. R., Anderson, R. S., Anderson, S. P., & Loso, M. G. (2005). Sediment evacuation and glacial erosion rates at a small alpine glacier. *Journal of Geophysical Research*, 110(F3). <https://doi.org/10.1029/2004JF000189>
- Rodriguez-Blanco, M. L., Soto-Varela, F., Taboada-Castro, M. M., & Taboada-Castro, M. T. (2018). Using hysteresis analysis to infer controls on sediment-associated and dissolved metals transport in a small humid temperate catchment. *Journal of Hydrology*, 565, 49–60. <https://doi.org/10.1016/j.jhydrol.2018.08.030>
- Rodriguez-Blanco, M. L., Taboada-Castro, M. M., Palleiro, L., & Taboada-Castro, M. T. (2010). Temporal changes in suspended sediment transport in an Atlantic catchment, NW Spain. *Geomorphology*, 123(1–2), 181–188. <https://doi.org/10.1016/j.geomorph.2010.07.015>
- Rose, L. A., & Karwan, D. L. (2021). Stormflow concentration-discharge dynamics of suspended sediment and dissolved phosphorus in an agricultural watershed. *Hydrological Processes*, 35(12). <https://doi.org/10.1002/hyp.14455>
- Rose, L. A., Karwan, D. L., & Godsey, S. E. (2018). Concentration-discharge relationships describe solute and sediment mobilization, reaction, and transport at event and longer timescales. *Hydrological Processes*, 32(18), 2829–2844. <https://doi.org/10.1002/hyp.13235>
- Rovira, A., & Batalla, R. J. (2006). Temporal distribution of suspended sediment transport in a Mediterranean basin: The Lower Tordera (NE Spain). *Geomorphology*, 79(1–2), 58–71. <https://doi.org/10.1016/j.geomorph.2005.09.016>
- Rustomji, P., Zhang, X. P., Hairsine, P. B., Zhang, L., & Zhao, J. (2008). River sediment load and concentration responses to changes in hydrology and catchment management in the Loess Plateau region of China. *Water Resources Research*, 44(7). <https://doi.org/10.1029/2007WR006656>
- Sadeghi, S. H. R., Ebrahimi Mohammadi, S., Singh, V. P., & Chapi, K. (2017). Non-point source contribution and dynamics of soluble and particulate phosphorus from main tributaries of the Zarivar Lake watershed, Iran. *Environmental Monitoring and Assessment*, 189(5), 238. Article 238. <https://doi.org/10.1007/s10661-017-5937-z>
- Sadeghi, S. H. R., Mizuyama, T., Miyata, S., Gomi, T., Kosugi, K., Fukushima, T., et al. (2008a). Determinant factors of sediment graphs and rating loops in a reforested watershed. *Journal of Hydrology*, 356(3–4), 271–282. <https://doi.org/10.1016/j.jhydrol.2008.04.005>
- Sadeghi, S. H. R., Mizuyama, T., Miyata, S., Gomi, T., Kosugi, K., Fukushima, T., et al. (2008b). Development, evaluation and interpretation of sediment rating curves for a Japanese small mountainous reforested watershed. *Geoderma*, 144(1–2), 198–211. <https://doi.org/10.1016/j.geoderma.2007.11.008>
- Sadeghi, S. H. R., & Saeidi, P. (2010). Reliability of sediment rating curves for a deciduous forest watershed in Iran. *Hydrological Sciences Journal*, 55(5), 821–831. <https://doi.org/10.1080/02626667.2010.489797>
- Sadeghi, S. H. R., Saeidi, P., Singh, V. P., & Telvari, A. R. (2019). How persistent are hysteresis patterns between suspended sediment concentration and discharge at different timescales? *Hydrological Sciences Journal*, 64(15), 1909–1917. <https://doi.org/10.1080/02626667.2019.1676895>
- Sadeghi, S. H. R., Singh, V. P., Kiani-Harchegani, M., & Asadi, H. (2018). Analysis of sediment rating loops and particle size distributions to characterize sediment source at mid-sized plot scale. *Catena*, 167, 221–227. <https://doi.org/10.1016/j.catena.2018.05.002>
- Safdar, R., Tahir, S., & Shahbaz, M. (2024). Urbanization and suspended sediment transport dynamics: A comparative study of watersheds with different land uses. *ACS ES&T Water*, 4(1), 334–344. <https://doi.org/10.1021/acsestwater.3c00328>
- Salant, N. L., Hassan, M. A., & Alonso, C. V. (2008). Suspended sediment dynamics at high and low storm flows in two small watersheds. *Hydrological Processes*, 22(11), 1573–1587. <https://doi.org/10.1002/hyp.6743>
- Sammori, T., Yusop, Z., Kasran, B., Noguchi, S., & Tani, M. (2004). Suspended solids discharge from a small forested basin in the humid tropics. *Hydrological Processes*, 18(4), 721–738. <https://doi.org/10.1002/hyp.1361>
- Serra, T., Soler, M., Barcelona, A., & Colomer, J. (2022). Suspended sediment transport and deposition in sediment-replenished artificial floods in Mediterranean rivers. *Journal of Hydrology*, 609, 127756. <https://doi.org/10.1016/j.jhydrol.2022.127756>
- Sherriff, S. C., Rowan, J. S., Fenton, O., Jordan, P., Melland, A. R., Mellander, P. E., & Huallachain, D. O. (2016). Storm event suspended sediment-discharge hysteresis and controls in agricultural watersheds: Implications for watershed scale sediment management. *Environmental Science & Technology*, 50(4), 1769–1778. <https://doi.org/10.1021/acs.est.5b04573>
- Shojaezadeh, S. A., Nikoo, M. R., Talebbeydokhti, N., Sadegh, M., & Adamowski, J. F. (2022). Process-constrained statistical modeling of sediment yield. *Catena*, 209, 105794. <https://doi.org/10.1016/j.catena.2021.105794>
- Sidle, R. C., & Campbell, A. J. (1985). Patterns of suspended sediment transport in a coastal Alaska stream. *JAWRA Journal of the American Water Resources Association*, 21(6), 909–917. <https://doi.org/10.1111/j.1752-1688.1985.tb00186.x>
- Singh, A. T., Sharma, P., Sharma, C., Laluraj, C. M., Patel, L., Pratap, B., et al. (2020). Water discharge and suspended sediment dynamics in the Chandra river, western Himalaya. *Journal of Earth System Science*, 129(1), 206. <https://doi.org/10.1007/s12040-020-01455-4>
- Smith, H. G., & Dragovich, D. (2009). Interpreting sediment delivery processes using suspended sediment-discharge hysteresis patterns from nested upland catchments, south-eastern Australia. *Hydrological Processes*, 23(17), 2415–2426. <https://doi.org/10.1002/hyp.7357>
- Soler, M., Latron, J., & Gallart, F. (2008). Relationships between suspended sediment concentrations and discharge in two small research basins in a mountainous Mediterranean area (Vallecebre, Eastern Pyrenees). *Geomorphology*, 98(1–2), 143–152. <https://doi.org/10.1016/j.geomorph.2007.02.032>
- Speir, S. L., Rose, L. A., Blaszcak, J. R., Kincaid, D. W., Fazekas, H. M., Webster, A. J., et al. (2024). Catchment concentration–discharge relationships across temporal scales: A review. *WIREs Water*, 11(2), e1702. <https://doi.org/10.1002/wat2.1702>

- Steegen, A., Govers, G., Nachtergaele, J., Takken, I., Beuselinck, L., & Poesen, J. (2000). Sediment export by water from an agricultural catchment in the Loam Belt of central Belgium. *Geomorphology*, 33(1–2), 25–36. [https://doi.org/10.1016/S0169-555X\(99\)00108-7](https://doi.org/10.1016/S0169-555X(99)00108-7)
- Strauch, A. M., MacKenzie, R. A., Giardina, C. P., & Bruland, G. L. (2018). Influence of declining mean annual rainfall on the behavior and yield of sediment and particulate organic carbon from tropical watersheds. *Geomorphology*, 306, 28–39. <https://doi.org/10.1016/j.geomorph.2017.12.030>
- Stubblefield, A. P., Reuter, J. E., Dahlgren, R. A., & Goldman, C. R. (2007). Use of turbidometry to characterize suspended sediment and phosphorus fluxes in the Lake Tahoe basin, California, USA. *Hydrological Processes*, 21(3), 281–291. <https://doi.org/10.1002/hyp.6234>
- Sun, L., Yan, M., Cai, Q., & Fang, H. (2016). Suspended sediment dynamics at different time scales in the Loushui River, south-central China. *Catena*, 136, 152–161. <https://doi.org/10.1016/j.catena.2015.02.014>
- Sun, X., Zhang, X., Fan, J., & Liu, L. (2024). Interpretation of suspended sediment concentration-runoff hysteresis loops in two small karst basins in Southwestern China. *Earth Surface Processes and Landforms*, 49(2), 236–248. <https://doi.org/10.1002/esp.5551>
- Swift, D. A., Tallentire, G. D., Farinotti, D., Cook, S. J., Higson, W. J., & Bryant, R. G. (2021). The hydrology of glacier-bed overdeepenings: Sediment transport mechanics, drainage system morphology, and geomorphological implications. *Earth Surface Processes and Landforms*, 46(11), 2264–2278. <https://doi.org/10.1002/esp.5173>
- Syvitski, J., Angel, J. R., Saito, Y., Overeem, I., Vorosmarty, C. J., Wang, H. J., & Olago, D. (2022). Earth's sediment cycle during the Anthropocene. *Nature Reviews Earth & Environment*, 3(3), 179–196. <https://doi.org/10.1038/s43017-021-00253-w>
- Tananaev, N. I. (2012). Hysteresis effect in the seasonal variations in the relationship between water discharge and suspended load in rivers of permafrost zone in Siberia and Far East. *Water Resources*, 39(6), 648–656. <https://doi.org/10.1134/S0097807812060073>
- Tananaev, N. I. (2015). Hysteresis effects of suspended sediment transport in relation to geomorphic conditions and dominant sediment sources in medium and large rivers of the Russian Arctic. *Hydrology Research*, 46(2), 232–243. <https://doi.org/10.2166/nh.2013.199>
- Tena, A., Vericat, D., & Batalla, R. J. (2014). Suspended sediment dynamics during flushing flows in a large impounded river (the lower River Ebro). *Journal of Soils and Sediments*, 14(12), 2057–2069. <https://doi.org/10.1007/s11368-014-0987-0>
- Tian, P., Zhai, J. Q., Zhao, G. J., & Mu, X. M. (2016). Dynamics of runoff and suspended sediment transport in a highly erodible catchment on the Chinese loess plateau. *Land Degradation & Development*, 27(3), 839–850. <https://doi.org/10.1002/ldr.2373>
- Tolorza, V., Carretier, S., Andermann, C., Ortega-Culaciati, F., Pinto, L., & Mardones, M. (2014). Contrasting mountain and piedmont dynamics of sediment discharge associated with groundwater storage variation in the Biobio River. *Journal of Geophysical Research-Earth Surface*, 119(12), 2730–2753. <https://doi.org/10.1002/2014JF003105>
- Tsyplenkov, A., Vanmaercke, M., Golosov, V., & Chalov, S. (2020). Suspended sediment budget and intra-event sediment dynamics of a small glaciated mountainous catchment in the Northern Caucasus. *Journal of Soils and Sediments*, 20(8), 3266–3281. <https://doi.org/10.1007/s11368-020-02633-z>
- Tuset, J., Vericat, D., Estany, D., & Batalla, R. J. (2022). Temporal patterns of suspended sediment dynamics in a Mediterranean mountainous catchment. *Zeitschrift für Geomorphologie*, 63(4), 379–405. <https://doi.org/10.1127/zfg/2022/0685>
- Upadhayay, H. R., Granger, S. J., & Collins, A. L. (2021). Dynamics of fluvial hydro-sedimentological, nutrient, particulate organic matter and effective particle size responses during the UK extreme wet winter of 2019–2020. *Science of the Total Environment*, 774, 145722. <https://doi.org/10.1016/j.scitotenv.2021.145722>
- Vale, S. S., & Dymond, J. R. (2020). Interpreting nested storm event suspended sediment-discharge hysteresis relationships at large catchment scales. *Hydrological Processes*, 34(2), 420–440. <https://doi.org/10.1002/hyp.13595>
- Valente, M. L., Reichert, J. M., Lopes Cavalcante, R. B., Gomes Minella, J. P., Evrard, O., & Srinivasan, R. (2021). Afforestation of degraded grasslands reduces sediment transport and may contribute to streamflow regulation in small catchments in the short-run. *Catena*, 204, 105371. <https://doi.org/10.1016/j.catena.2021.105371>
- Varvani, J., Khaleghi, M. R., & Gholami, V. (2019). Investigation of the relationship between sediment graph and hydrograph of flood events (Case study: Gharachay River tributaries, Arak, Iran). *Water Resources*, 46(6), 883–893. <https://doi.org/10.1134/S0097807819050157>
- Vaughan, M. C. H., Bowden, W. B., Shanley, J. B., Vermilyea, A., Sleeper, R., Gold, A. J., et al. (2017). High-frequency dissolved organic carbon and nitrate measurements reveal differences in storm hysteresis and loading in relation to land cover and seasonality. *Water Resources Research*, 53(7), 5345–5363. <https://doi.org/10.1002/2017WR020491>
- Vercruyse, K., & Grabowski, R. C. (2019). Temporal variation in suspended sediment transport: Linking sediment sources and hydro-meteorological drivers. *Earth Surface Processes and Landforms*, 44(13), 2587–2599. <https://doi.org/10.1002/esp.4682>
- Vercruyse, K., Grabowski, R. C., & Rickson, R. J. (2017). Suspended sediment transport dynamics in rivers: Multi-scale drivers of temporal variation. *Earth-Science Reviews*, 166, 38–52. <https://doi.org/10.1016/j.earscirev.2016.12.016>
- Walling, D. E. (1977). Assessing the accuracy of suspended sediment rating curves for a small basin. *Water Resources Research*, 13(3), 531–538. <https://doi.org/10.1029/WR013i003p00531>
- Walling, D. E. (2006). Human impact on land-ocean sediment transfer by the world's rivers. *Geomorphology*, 79(3–4), 192–216. <https://doi.org/10.1016/j.geomorph.2006.06.019>
- Wang, B., Wang, C., Jia, B., & Fu, X. (2022). Spatial variation of event-based suspended sediment dynamics in the middle Yellow River basin, China. *Geomorphology*, 401, 108115. <https://doi.org/10.1016/j.geomorph.2022.108115>
- Weng, H., Barneveld, R., Bechmann, M., Marttila, H., Krogstad, T., & Skarbovik, E. (2021). Sediment transport dynamics in small agricultural catchments in a cold climate: A case study from Norway. *Agriculture, Ecosystems & Environment*, 317, 317. <https://doi.org/10.1016/j.agee.2021.107484>
- Whiting, P. J., Stamm, J. F., Moog, D. B., & Orndorff, R. L. (1999). Sediment-transporting flows in headwater streams. *GSA Bulletin*, 111(3), 450–466. [https://doi.org/10.1130/0016-7606\(1999\)111<0450:STFIHS>2.3.CO;2](https://doi.org/10.1130/0016-7606(1999)111<0450:STFIHS>2.3.CO;2)
- Wilcox, J. D., Stark, K. A., & Svetlov, R. (2024). Estimating stream sediment loads to assess management options for a Southern Appalachian mountain lake. *Environmental Earth Sciences*, 83(13), 387. <https://doi.org/10.1007/s12665-024-11677-0>
- Williams, G. P. (1989). Sediment concentration versus water discharge during single hydrologic events in rivers. *Journal of Hydrology*, 111(1–4), 89–106. [https://doi.org/10.1016/0022-1694\(89\)90254-0](https://doi.org/10.1016/0022-1694(89)90254-0)
- Wilson, C. G., Papanicolaou, A. N. T., & Denn, K. D. (2012). Partitioning fine sediment loads in a headwater system with intensive agriculture. *Journal of Soils and Sediments*, 12(6), 966–981. <https://doi.org/10.1007/s11368-012-0504-2>
- Wood, P. A. (1977). Controls of variation in suspended sediment concentration in the river Rother, west Sussex, England. *Sedimentology*, 24(3), 437–445. <https://doi.org/10.1111/j.1365-3091.1977.tb00131.x>
- Wymore, A. S., Leon, M. C., Shanley, J. B., & McDowell, W. H. (2019). Hysteretic response of solutes and turbidity at the event scale across forested tropical Montane watersheds. *Frontiers in Earth Science*, 7. <https://doi.org/10.3389/feart.2019.00126>
- Xiao, Y., Qian, Y., & Li, M. (2024). Suspended sediment dynamics and linking with watershed surface characteristics in a karst region. *Journal of Hydrology*, 622, 129328. <https://doi.org/10.1016/j.jhydrol.2023.129328>

- Xue, Z., Li, Q., & Yang, W. (2024). Characteristics of runoff and sediment transport during flood events in the upper Yangtze river. *Journal of Environmental Management*, 339, 117004. <https://doi.org/10.1016/j.jenvman.2023.117004>
- Yang, C. C., & Lee, K. T. (2018). Analysis of flow-sediment rating curve hysteresis based on flow and sediment travel time estimations. *International Journal of Sediment Research*, 33(2), 171–182. <https://doi.org/10.1016/j.ijsrc.2017.10.003>
- Yeshaneh, E., Eder, A., & Bloeschl, G. (2014). Temporal variation of suspended sediment transport in the Koga catchment, North Western Ethiopia and environmental implications. *Hydrological Processes*, 28(24), 5972–5984. <https://doi.org/10.1002/hyp.10090>
- Yibeltal, M., Tsunekawa, A., Haregeweyn, N., Adgo, E., Meshesha, D. T., Zegeye, A. D., et al. (2023). Analyzing the contribution of gully erosion to land degradation in the upper Blue Nile basin, Ethiopia. *Journal of Environmental Management*, 344, 118378. <https://doi.org/10.1016/j.jenvman.2023.118378>
- Yu, B., Shi, Z., & Zhang, Y. (2023). Linking hydrological and landscape characteristics to suspended sediment-discharge hysteresis in Wudinghe River Basin on the Loess Plateau, China. *Catena*, 228, 107169. <https://doi.org/10.1016/j.catena.2023.107169>
- Yu, G. A., Li, Z., Disse, M., & Huang, H. Q. (2017). Sediment dynamics of an allogenic river channel in a very arid environment. *Hydrological Processes*, 31(11), 2050–2061. <https://doi.org/10.1002/hyp.11171>
- Zarnaghsh, A., & Husic, A. (2021). Degree of anthropogenic land disturbance controls fluvial sediment hysteresis. *Environmental Science & Technology*, 55(20), 13737–13748. <https://doi.org/10.1021/acs.est.1c00740>
- Zarnaghsh, A., & Husic, A. (2023). An index for inferring dominant transport pathways of solutes and sediment: Assessing land use impacts with high-frequency conductivity and turbidity sensor data. *Science of the Total Environment*, 894, 164931. <https://doi.org/10.1016/j.scitotenv.2023.164931>
- Zhao, G., Yue, X., Tian, P., Mu, X., Xu, W., Wang, F., et al. (2017). Comparison of the suspended sediment dynamics in two loess plateau catchments, China. *Land Degradation & Development*, 28(4), 1398–1411. <https://doi.org/10.1002/ldr.2645>
- Zhou, Y. W., Li, Z. X., Wang, T. W., Wang, J., Deng, J., Du, Y. N., et al. (2023). Divergent hydrological responses to intensive production under different rainfall regimes: Evidence from long-term field observations. *Journal of Hydrology*, 617, 128918. <https://doi.org/10.1016/j.jhydrol.2022.128918>
- Zhu, M., Li, Z., Xu, X., & Ye, Z. (2023). Quantifying and interpreting the hysteresis patterns of monthly sediment concentration and water discharge in karst watersheds. *Journal of Hydrology*, 618, 129179. <https://doi.org/10.1016/j.jhydrol.2023.129179>
- Ziegler, A. D., Benner, S. G., Tantasirin, C., Wood, S. H., Sutherland, R. A., Sidle, R. C., et al. (2014). Turbidity-based sediment monitoring in northern Thailand: Hysteresis, variability, and uncertainty. *Journal of Hydrology*, 519, 2020–2039. <https://doi.org/10.1016/j.jhydrol.2014.09.010>
- Zou, Y. W., Huang, X., Hou, M. T., & She, D. L. (2022). Linking watershed hydrologic processes to connectivity indices on the Loess Plateau, China. *Catena*, 216, 106341. <https://doi.org/10.1016/j.catena.2022.106341>
- Zuocco, G., Penna, D., Borga, M., & van Meerveld, H. J. (2016). A versatile index to characterize hysteresis between hydrological variables at the runoff event timescale. *Hydrological Processes*, 30(9), 1449–1466. <https://doi.org/10.1002/hyp.10681>